CHAPTER 4

Results and Discussion

4.1 Properties of Active-Coated Papers

4.1.1 Thickness

The thickness are remarkable parameters, which can affect the functional and mechanical properties of biopolymer-coated paper (Gällstedt & Hedenqvist, 2004; Gällstedt, Brottman, & Hedenqvist, 2005). For this study, the uncoated paper and the paper coated with chitosan and carboxymethyl cellulose (CMC) were in short called as UNC, VCS 0.0 and VCMC 0.0, respectively. While, papers coated by chitosan-based coatings with 0.5, 1.0, 2.0 and 4.0 (w/v) concentrations of vanillin were in short called as VCS 0.5, VCS 1.0, VCS 2.0 and VCS 4.0, respectively. Likewise, papers coated by CMC-based coatings with 0.5, 1.0, 2.0 and 4.0 (w/v) concentrations of vanillin were in short called as VCMC 0.5, VCMC 1.0, VCMC 2.0 and VCMC 4.0, respectively. As shown in Table 4.1, the thickness of all the papers was in the range of 39 to 48 μm. The coating process clearly increased the thickness of UNC. Both VCS 0.0 (41 μm) and VCMC 0.0 (42 μm) showed the higher thickness than UNC, which was only 39 μm ($p \leq 0.05$). Although an increase in vanillin concentration did not affect the thickness of all the coated papers incorporating with vanillin ($p > 0.05$), but the addition of vanillin exceeding 2 % gave the significantly higher thickness than those of VCS 0.0 or VCMC 0.0 without vanillin addition ($p \leq 0.05$).

4.1.2 Moisture Content

Moisture content can influence the stability of various paper properties such as the thickness, barrier and mechanical properties. As seen in Table 4.1, the UNC showed the lowest moisture content (6.25 %) in this study, followed by VCS 0.0 (7.36 %) and VCMC 0.0 (9.17 %) ($p \leq 0.05$). While, the addition of vanillin was not effect on the moisture content of paper ($p > 0.05$). This result might be due to the water absorption of each biopolymer. For UNC, cellulose is its major component which is hygroscopic in nature and

can absorb some moisture from the atmosphere. The coating process caused an increase in hygroscopic surface due to the increment of thickness, hygroscopic surface area, and ability to absorb. Chitosan and CMC contains hydrophilic groups, which contributed to their higher moisture absorption than only cellulose-based UNC. More than the increase in the hygroscopic surface area, the chitosan layer could absorb the water vapors from surrounding wet atmosphere and held them in the film, leading to higher moisture content. It is well-known that the formation of hydrogen bond linked between hydroxyl/amino groups of chitosan and water molecule can be occurred (Khan, Peh, & Ch'ng, 2002; Denuziere, Ferrier, Damour, & Domard, 1998). Similar to chitosan, hydroxyl and carboxyl groups of CMC layer were the key functional groups that could also form a hydrogen bond with a water molecule, resulting in higher moisture content of the coated paper.

4.1.3 Color

Table 4.1 represents L^*, a^* and b^* of coated papers with varying coating materials and vanillin concentrations. The L^* represents the lightness or darkness of the paper. The values are always ranging from 0-100. Black is 0 and 100 is white. It was found that L^* of UNC, VCS 0.0 and VCMC 0.0 was not significantly different ($p \leq 0.05$). The values were ranged from 87.59 to 87.74. However, the difference is not significant hence both chitosan and CMC had no effect on paper brightness. The L^* values slightly decreased with increasing vanillin concentrations. Yellow is the brightest color to the human eye, because of it generally has high saturation and high brightness values, therefore its brightness is closed to white. The a^* value represents the redness color of paper while b^* value represents the yellowish color of paper. An increase in the b^* value indicates that the color of the paper is becoming more yellow. According to Table 4.1, it was found that coating solutions did not significantly alter a^* and b^* value of paper. The a^* and b^* value of UNC were 0.38 and 5.61, respectively while a^* and b^* were 0.28 and 5.82, respectively for VCS 0.0 and were 0.31 and 5.76, respectively for VCMC 0.0. However, the b^* value was significantly increased with vanillin addition and the increase was significant with each incremental increase in vanillin. Sangsuwan et al. (2008) found that the increasing of vanillin concentration led to an enhancement of the yellowness of chitosan/methylcellulose films.

Table 4.1 Thickness, coating weight, moisture content, and color of active-coated papers prepared from various coating materials and vanillin concentrations

Samples	Thickness (μm)	Moisture content (%)	*L**	*a**	*b**
UNC	39 ^{d} ± 2	6.25 ^{c} ± 0.36	87.74 ^{a} ± 0.24	0.38 ^{a} ± 0.02	5.61 ^{i} ± 0.20
VCS 0.0	41 ^{cd} ± 3	7.36 ^{b} ± 0.23	87.59 ^{ab} ± 0.07	0.28 ^{a} ± 0.05	5.82 ^{i} ± 0.16
VCS 0.5	44 ^{abc} ± 3	7.50 ^{b} ± 0.46	87.41 ^{cd} ± 0.11	-3.41 ^{c} ± 0.20	14.67 ^{g} ± 0.18
VCS 1.0	45 ^{abc} ± 2	7.61 ^{b} ± 0.12	87.28 ^{d} ± 0.08	-4.24 ^{e} ± 0.16	19.79 ^{e} ± 0.19
VCS 2.0	46 ^{ab} ± 3	7.42 ^{b} ± 0.24	86.61 ^{f} ± 0.14	-4.58 ^{f} ± 0.17	26.65 ^{c} ± 0.20
VCS 4.0	47 ^{a} ± 1	7.32 ^{b} ± 0.14	86.44 ^{g} ± 0.09	-4.87 ^{g} ± 0.12	33.36 ^{a} ± 0.12
VCMC 0.0	42 ^{bc} ± 2	9.17 ^{a} ± 0.28	87.64 ^{a} ± 0.13	0.31 ^{a} ± 0.02	5.76 ^{i} ± 0.12
VCMC 0.5	45 ^{abc} ± 2	9.38 ^{a} ± 0.36	87.46 ^{bc} ± 0.07	-3.17 ^{b} ± 0.17	13.07 ^{h} ± 0.15
VCMC 1.0	45 ^{ab} ± 1	9.52 ^{a} ± 0.15	87.36 ^{cd} ± 0.12	-3.94 ^{d} ± 0.17	17.73 ^{f} ± 0.14
VCMC 2.0	46 ^{a} ± 1	9.22 ^{a} ± 0.28	86.81 ^{e} ± 0.11	-4.36 ^{e} ± 0.08	24.65 ^{d} ± 0.17
VCMC 4.0	48 ^{a} ± 1	9.14 ^{a} ± 0.15	86.58 ^{fg} ± 0.12	-4.66 ^{f} ± 0.10	31.75 ^{b} ± 0.15

Superscript letters in each column indicated significantly difference at $p \leq 0.05$.

4.1.4 Water Vapor Permeability

The water vapor permeability (WVP) value is an important determinant related to the hydrophilic fraction of the film, therefore more hydrophilic films will have the greater WVP (Zivanovic, Chi, & Draughon, 2005; Tongdeesoontorn, Mauer, Wongruong, & Rachtanapun, 2009). As shown in Table 4.2, WVP values of all coated papers were lower than UNC ($p \leq 0.05$). Without the vanillin addition, paper coated with chitosan (VCS 0.0) had the significantly lower WVP (1.34×10^{-4} g/m^2·day·Pa) than paper coated with CMC (VCMC 0.0) (3.24×10^{-4} g/m^2·day·Pa) ($p \leq 0.05$). These results obtained might be attributed to the semi-crystalline nature of chitosan, which is one of a key factor affecting its mechanical and functional properties (Nicu, Bobu, & Desbrieres, 2011). In a solid state, chitosan molecules organize themselves into ordered crystalline regions co-existing in an amorphous phase (Samuels, 1981). Thus it was more difficult for water molecule to penetrate through the crystalline regions inside the film layer of chitosan-coated paper. The film prepared from chitosan has moderate WVP in which it can be used to protect the water loss of fresh produce and foodstuffs with higher water activity values (Khwaldia, Arab-Tehrany, & Desobry, 2010). For VCMC 0.0, this study demonstrated that the paper surface coated with CMC was a poor water vapor barrier because of most compositions of CMC consisted of hydrophilic polysaccharides with numerous hydroxyl groups, which could form the hydrogen bond, leading to easier absorb the water molecule. Thus, the WVP values of VCMC 0.0 were higher than VCS 0.0.

Additionally, the incorporation of vanillin into the coating solution could reduce the barrier against water vapor (Table 4.2). It was found that WVP values of VCS 0.0 decreased from 1.34×10^{-4} to 0.58×10^{-4} g/m^2·day·Pa by increasing the concentration of vanillin from 0.5 to 4.0 %. Likewise, WVP values of VCMC 0.0 decreased from 3.24×10^{-4} to 1.84×10^{-4} g/m^2·day·Pa by increasing the concentration of vanillin from 0.5 to 4.0 %. Because vanillin are hydrophobic, the increase in hydrophobicity of the film matrix should reduce water absorption. Similarly, water vapor permeability decreased with increased fraction of the hydrophobic compound. This behavior was observed, for example, with oleic acid in CMC films and palm olein in CMC/glucomannan blend films (Cheng et al., 2008; Ghanbarzadeh & Almasi, 2011). This observation is in parallel with another study where a paper coating of chitosan-palmitic acid blends resulted in improvement in WVP (Bordenave, Grelier, Pichavant & Coma, 2010).

Table 4.2 Water vapor permeability, tensile strength, and elongation of coated papers prepared from various coating materials and vanillin concentrations

Samples	WVP ($\times 10^{-4}$ g/ m^2.day Pa)	Tensile strength (MPa)	Elongation (%)
UNC	$3.51^{a} \pm 0.24$	$56.18^{e} \pm 1.79$	$1.68^{e} \pm 0.13$
VCS 0.0	$1.34^{f} \pm 0.03$	$62.43^{a} \pm 2.21$	$2.86^{a} \pm 0.22$
VCS 0.5	$1.31^{f} \pm 0.19$	$58.89^{b} \pm 1.43$	$2.68^{abc} \pm 0.18$
VCS 1.0	$0.61^{g} \pm 0.06$	$58.57^{bc} \pm 1.86$	$2.57^{c} \pm 0.14$
VCS 2.0	$0.59^{g} \pm 0.05$	$57.27^{bcde} \pm 1.32$	$2.28^{d} \pm 0.14$
VCS 4.0	$0.58^{g} \pm 0.04$	$56.50^{de} \pm 1.95$	$2.19^{d} \pm 0.12$
VCMC 0.0	$3.24^{b} \pm 0.14$	$58.35^{bcd} \pm 2.84$	$2.83^{ab} \pm 0.46$
VCMC 0.5	$2.42^{c} \pm 0.19$	$57.77^{bcde} \pm 2.48$	$2.63^{bc} \pm 0.29$
VCMC 1.0	$2.14^{d} \pm 0.14$	$57.27^{bcde} \pm 2.84$	$2.52^{c} \pm 0.09$
VCMC 2.0	$1.86^{e} \pm 0.14$	$56.79^{cde} \pm 1.37$	$2.24^{d} \pm 0.12$
VCMC 4.0	$1.84^{e} \pm 0.10$	$56.31^{de} \pm 1.16$	$2.17^{d} \pm 0.28$

Superscript letters in each column indicated significantly difference at $p \leq 0.05$.

4.1.5 Tensile Strength and Percent Elongation

As shown in Table 4.2, it was found that the tensile strength and elongation of all the coated papers were higher than UNC. The paper coated with chitosan (63.43 MPa) had the greater tensile strength than which of CMC (58.35 MPa) ($p \leq 0.05$), whereas the elongations of VCS 0.0 (2.86 %) and VCMC 0.0 (2.83 %) were not significantly different ($p > 0.05$). In addition, the result also indicated that the coating process by all of the coating solutions could improve the tensile strength and elongation of coated papers. Especially its elongation that the significant difference was clearly seen. The result may be due to the charge difference of chitosan and cellulose-based substrate, which can be expected to yield good adhesion and dense layer on the surface of coated paper (Wang & Jing, 2016; Khwaldia et al., 2010). The positive charges of chitosan at the interface between

coating layer and paper surface might be electrostatically interacted with negative charges of the paper's cellulose fiber, resulting in the tensile strength of VCS 0.0 were higher than VCMC 0.0. The results are consistent with those of Vartiainen et al. (2004), the authors reported that chitosan coating could improve the tensile strength and elongation due to the formation of tough, flexible, and tear-resistant films, acted as a reinforcement layer. Additionally, chitosan has also been used as a wet end additive in paperboard and the mechanical properties of the product were reported to be improved (Laleg & Pikulik, 1991).

As seen in Table 4.2, tensile strength and elongation of all the coated papers had a tendency to decrease, when the vanillin concentration increased. Its tensile strength and elongation of chitosan-coated papers decreased from 62.43 to 56.50 MPa and 2.86 to 2.19 %, respectively. Likewise, the tensile strength and elongation of CMC-coated papers decreased from 58.35 to 56.31 MPa and 2.83 to 2.17 %, respectively. Incorporation of vanillin into the film changed the functional characteristics of the packaging materials. The molecular structure of vanillin is composed of an aromatic benzene ring like styrene monomer. The bulky structure of vanillin made the film more rigid and contributed to the loss of its segmental mobility (Birley, Haworth, & Batchelor, 1992). These could explain the results in decreased tensile strength and elongation when vanillin was introduced into coated papers. The result conformed to Sangsuwan et al. (2008), the authors demonstrated that the incorporation of vanillin to the chitosan/methylcellulose film decreased the elongation and the decrease continued as the vanillin level increased.

4.1.6 Surface Morphology

The surface morphology of all the papers is shown in Figure 4.1 and 4.2. They demonstrated that UNC had rough surface with fibers crossed to each other and had lots of pores. In a coating process, microporous pores on the paper surface were filled with a coating solution, which was formed as a layer of film. Therefore, the coated paper had smoother surface compared with uncoated paper. Based on SEM micrograph, it was showed that both chitosan and CMC provided a uniformity thin film on the surface of paper. In Figure 4.1, the solubility of vanillin in water was limited by its concentration at 1.0 %. It could be obviously observed the vanillin crystal on the surface of paper coated with vanillin 2.0 and 4.0 % (w/v). The vanillin crystals were observed in both the chitosan and CMC-coated papers.

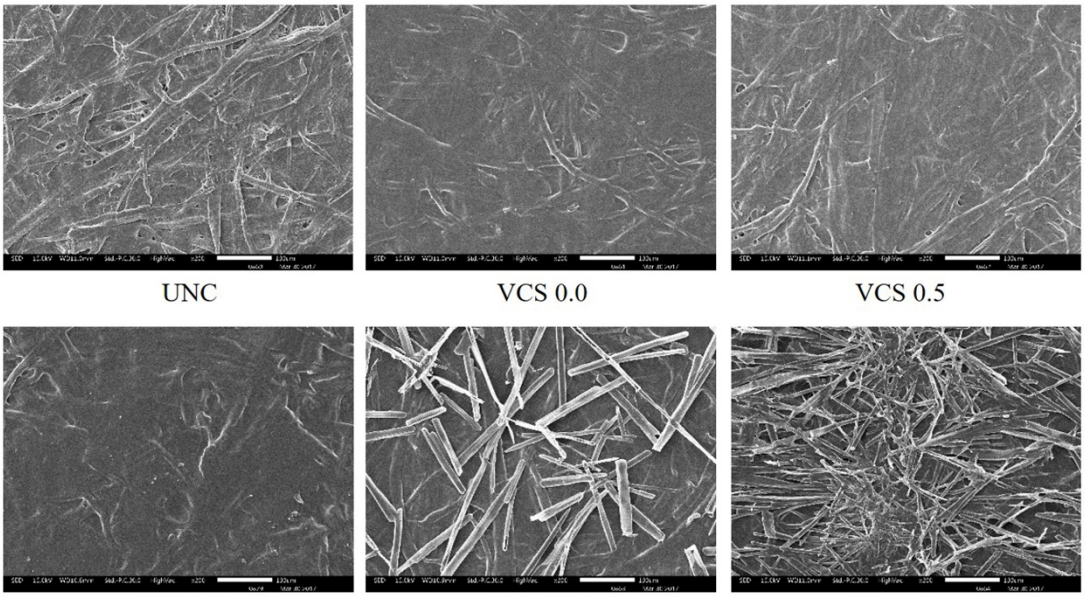

Figure 4.1 Surface topography of uncoated paper (UNC), chitosan-coated paper (VCS 0.0), and vanillin-chitosan coated papers containing 0.5, 1.0, 2.0 and 4.0 % (w/v) of vanillin (VCS 0.5, VCS 1.0, VCS 2.0 and VCS 4.0, respectively) at the magnification of 200×.

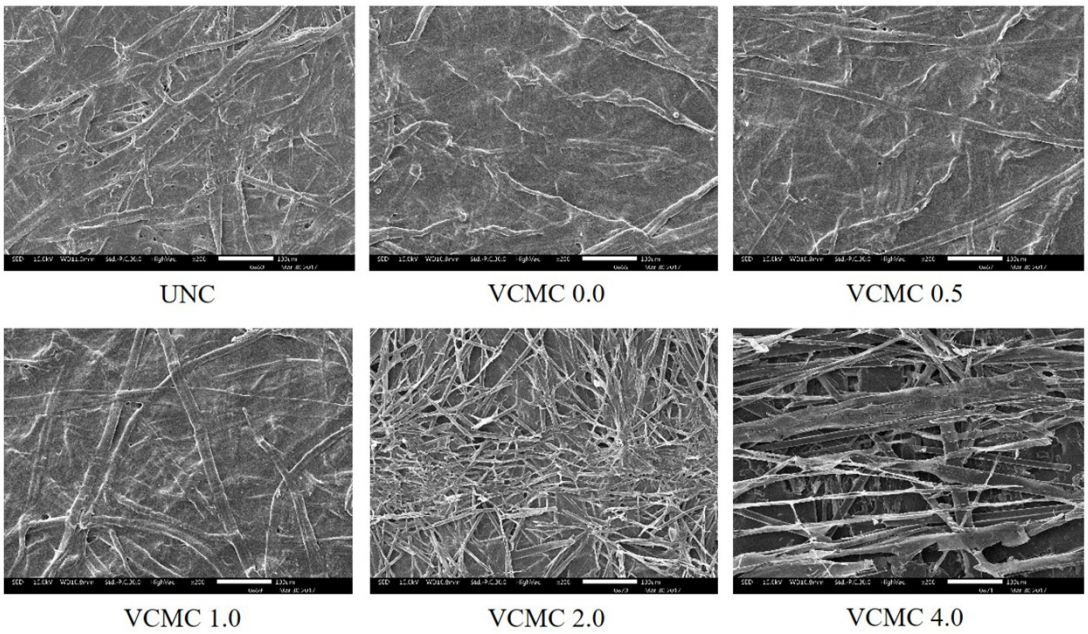

Figure 4.2 Surface topography of uncoated paper (UNC), CMC-coated paper (VCMC 0.0), and vanillin-CMC coated papers containing 0.5, 1.0, 2.0 and 4.0 % (w/v) of vanillin (VCMC 0.5, VCMC 1.0, VCMC 2.0 and VCMC 4.0, respectively) at the magnification of 200×.

4.2 Efficacy of Vanillin-Coated Papers against Anthracnose Fungi of Mango Fruits

4.2.1 Characteristics of Mycelia and Conidiospores Isolated from Anthracnose Infected Mango Fruits

The symptom of the anthracnose-infected mango fruits *cv* Nam Dok Mai caused by *C. gloeosporioides* was shown in Figure 4.3. Lesions on the infected mango fruit surface appeared as rounded brown to black circles with an indefinite border and size. Most of lesions were deflated and shriveled characteristics. Lesions larger than 1.0 cm were normally found around the fruit, afterward, different size of those lesions could coalesce and expanded until it covered the most area of mango fruits. As seen in Figure 4.3, the arrowheads indicated that these anthracnose-infected mango fruits were in the advanced stage of disease. Because of *C. gloeosporioides* produced masses of orange conidiospores inside the central circle of the lesions. Additionally, these lesions were not only restricted on the peel of infected mango fruits, but this stage the fungus could also invade into its flesh.

Figure 4.3 The symptom of mango *cv* Nam Dok Mai fruits infected anthracnose caused by *C. gloeosporioides*.

Afterward, *C. gloeosporioides* were isolated by a tissue transplanting method on a potato dextrose agar (PDA) for 72 h. The result of fungal cultures observed that the fungus could grow out from anthracnose-infected mango fruit tissues and produced abundant mycelia. The mycelia of these fungal colonies are consisted of a network of fine white

to grey filaments (Figure 4.4 (A)). During the incubation, fungal masses of orange conidiospores were widely formed on their mycelia, as shown in Figure 4.4 (B).

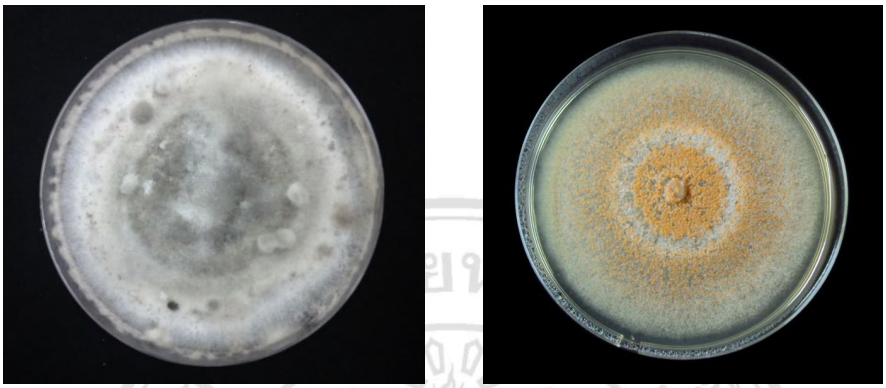

(A) (B)

Figure 4.4 Characteristics of mycelia and conidiospores of *C. gloeosporioides* grew on PDA media; Characteristics of *C. gloeosporioides*'s mycelia (A) and of *C. gloeosporioides*'s orange conidiospores formed on their mycelia (B).

For *C. gloeosporioides*'s conidiospores, they were collected from region of orange strip to use for evaluating their characteristics. The result found that conidiospores of the isolates under a light microscope with 400× magnificent showed as single spores with ovoid to oblong and slightly curved (Figure 4.5).

Figure 4.5 Characteristics of *C. gloeosporioides*'s conidiospores under a light microscope with 100× magnificent.

4.2.2 Efficacy of Active Coating Solutions against Mango Anthracnose Fungi

1) Inhibitory effects of active coating solutions against mycelial growths of mango anthracnose fungi

The MIC test was selected for evaluating the inhibition efficacy of each active coating solution against anthracnose fungi in mango fruits. In this experiment, vanillin (4-Hydroxy-3-methoxybenzaldehyde) as semi-volatile phenolic compound was selected to be applied as an active substance for inhibiting the anthracnose fungi due to its antifungal activities, which have been reported by previous researches (Lopez-Malo et al., 1995; Lopez-Malo et al., 1997; Sangsuwan et al., 2008). Additionally, the negative effects in associated with its flavor on the consumer acceptance in mango flesh were not found. Various vanillin concentrations (0.5, 1.0, 2.0, and 4.0 %, w/v) incorporating into either chitosan or carboxymethyl cellulose coating solutions were individually prepared. For each treatment, chitosan or CMC incorporating with vanillin at different concentrations (0.5, 1.0, 2.0 and 4.0 %, w/v). Chitosan and CMC coating solution were in short called as VCS 0.0 and VCMC 0.0, respectively. While, chitosan coating solution with 0.5, 1.0, 2.0 and 4.0 (w/v) concentrations of vanillin were in short called as VCS 0.5, VCS 1.0, VCS 2.0 and VCS 4.0, respectively. Likewise, CMC coating solution with 0.5, 1.0, 2.0 and 4.0 (w/v) concentrations of vanillin were in short called as VCMC 0.5, VCMC 1.0, VCMC 2.0 and VCMC 4.0, respectively. The inhibitory effect of each treatment against mycelial growths of *C. gloeosporioides* isolated from the mango fruit was verified and compared with a control without addition of any coating solution. All of coating solutions were investigated by dropped onto the mycelia of *C. gloeosporioides*'s colonies, cultured on PDA medium at 25 ± 2 °C for 24 h, and then incubated at a room temperature (25 ± 2 °C) for 7 days.

After the incubation, the results of this experiment are shown in Figure 4.6 to 4.7. In the control, *C. gloeosporioides* could be fully grown on PDA medium without coating solutions, indicating that there were not inhibitory effects found in this plate. Likewise, acetic acid solution (1 %, v/v), which is the solution used for chitosan preparation, could not be inhibited the mycelial growth of anthracnose fungi as same as the control. As shown in Figure 4.6, this experimental result showed that all concentrations of vanillin-chitosan coating solutions could inhibit the mycelial growth of anthracnose fungi in mango fruits, and their inhibitory effects were obviously greater than VCS 0.0 itself. The fungus

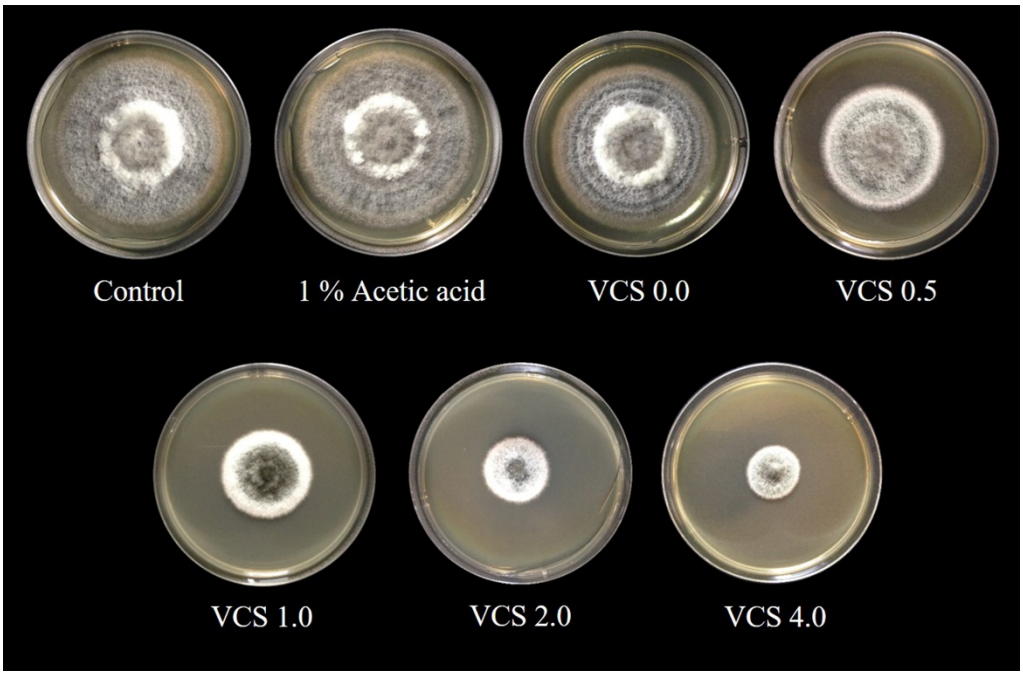

Figure 4.6 Inhibitory effects of vanillin-chitosan coating solutions against the mycelial growth of *C. gloeosporioides* cultured on PDA medium for 7 days.

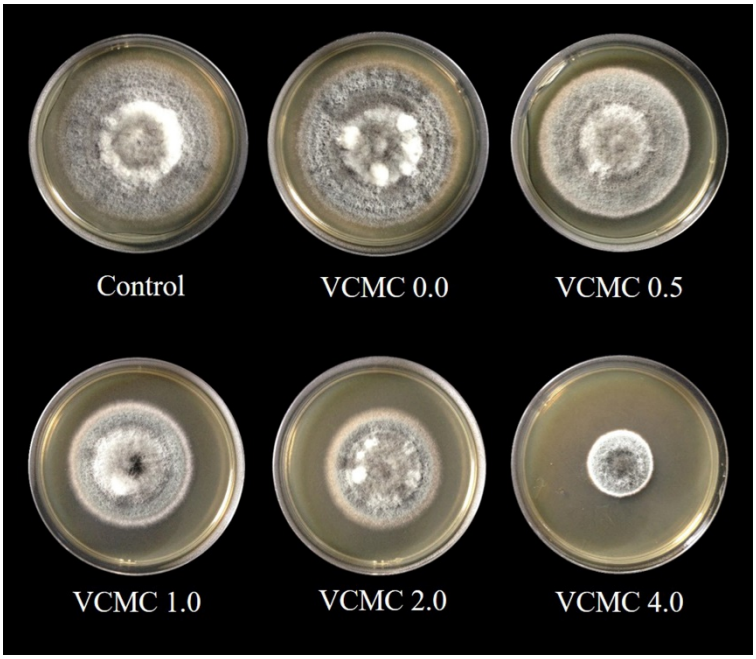

Figure 4.7 Inhibitory effects of vanillin-CMC coating solutions against the mycelial growth of *C. gloeosporioides* cultured on PDA medium for 7 days.

could be greatly grown in VCS 0.5, judged by its biggest colony size, which respectively reduced by increasing the concentration of vanillin. The smallest fungal colony size was observed at VCS 4.0. Likewise, the experimental result testing with vanillin-CMC coating solutions was shown in Figure 4.7. The lowest inhibitory effect was observed in the VCMC 0.5 due to its larger colony size, but this concentration provided higher inhibitory effects than both of control and VCMC 0.0.

For VCMC 0.0, it had no inhibitory effects against anthracnose fungus at all. The fungal colony size in CMC treatment and control were similar and abundant orange spores of the fungus were commonly formed in both CMC treatment and control. In contrary to the inhibitory effects of vanillin-chitosan coating solutions, the fungal colony size was respectively decreased by increasing vanillin concentrations. The best inhibitory effect with the smallest fungal colony size was observed in VCMC 4.0. Moreover, the inhibitory effect could also be expressed as the percent inhibition of radical growth (PIRG), which was calculated by Equation (4.1).

$$\text{PIRG (\%)} = \left(\frac{x - y}{x} \right) \times 100 \qquad (4.1)$$

Where, x is the colony size of *C. gloeosporioides* grown on control plate.
y is the colony size of *C. gloeosporioides* grown on treatment plate.

As shown in Table 4.3, the VCS 4.0 gave the highest PIRG (83.25 %), which was significantly greater than other treatments ($p \leq 0.05$), followed by VCS 2.0, VCS 1.0, VCS 0.5, and VCS 0.0, respectively. Comparing with VCS 0.0, the VCS 4.0 exhibited the greater inhibitory effect than the VCS 0.0 for 56.42 %. This result indicated that the inhibitory effect of vanillin-chitosan coating solutions was dependent on the concentration of vanillin. Increasing the vanillin concentrations also enhanced the PIRG. Without addition of vanillin, the CHI could inhibit the radical growth of mango anthracnose fungal mycelia for 26.83 % only. The molecular structure of chitosan containing a larger number of amino group ($-NH_2$), which can absorb hydrogen ions from the surrounding solution and formed

Table 4.3 The PIRG of *C. gloeosporioides* cultured on PDA for 7 days evaluated by the drop test technique.

Treatments	PIRG (%)	Treatments	PIRG (%)
VCS 0.0	26.83 ^{eA} ± 0.71	VCMC 0.0	00.00 ^{eB} ± 0.00
VCS 0.5	42.08 ^{dA} ± 0.35	VCMC 0.5	29.17 ^{dB} ± 0.59
VCS 1.0	62.08 ^{cA} ± 0.59	VCMC 1.0	50.79 ^{cB} ± 0.65
VCS 2.0	75.54 ^{bA} ± 0.29	VCMC 2.0	57.92 ^{bB} ± 0.82
VCS 4.0	83.25 ^{aA} ± 0.12	VCMC 4.0	69.08 ^{aB} ± 0.24
1 % Acetic acid	2.75 ^{f} ± 0.35	-	-

Data shows the average ± standard deviation of three replications (n = 3).
Different lower case superscript letters in each column indicate significantly different at $p \leq 0.05$.
Different upper case superscript letters in each row indicate significantly different at $p \leq 0.05$.

as the ammonium ion ($-NH_3^+$) (Xie, Xu, & Liu, 2001). The electrostatic interaction between a positive charge of ammonium groups of chitosan and a negative charge of phosphoryl groups of phospholipids on the microorganism's cell membrane at pH < 6.3 is occurred and leading to the leakage of various ions, such as, K^+, H^+, Ca^{2+}, and Cl^- and other inside components (Liu et al., 2004). Hence, this interaction may be an important mechanism of chitosan causing alteration in membrane permeability for this experiment and finally led to cell death (Papineau, Hoover, Knorr, & Farkas, 1991; Li et al., 2010).

The lower inhibitory effect was observed in the vanillin-CMC coating solution. As seen in Table 4.3, the VCMC 4.0 gave the highest PIRG (69.08 %), which was significantly greater than other treatments ($p \leq 0.05$), followed by VCMC 2.0, VCMC 1.0, VCMC 0.5, and VCMC 0.0, respectively. Comparing with VCMC 0.0, VCMC 4.0 showed the greater inhibitory effect than VCMC 0.0 for 100 %. This obviously demonstrated that only CMC could not inhibit mycelial growth of anthracnose fungi in mango fruits. However, the antifungal activities of CMC against some species, *i.e.*, *Aspergillus flavus*, have also been reported (El-Sherbiny, Salama, & Sarhan, 2009). Such antifungal effects of CMC caused by enhancing of sodium ion (Na^+). Higher Na^+ directly altered ion hemostasis, resulting in hyperosmotic stress, ionic imbalance, and toxicity (Niu, Bressan, Hasegawa, &

Pardo, 1995). Although CMC had no antifungal effects in this study, but it might be act as a good carrier facilitating vanillin diffusions. Inhibitory effects of vanillin-CMC coating solution directly related to the vanillin concentration, and enhanced by increasing concentrations of vanillin.

Furthermore, this experiment also demonstrated that both vanillin-chitosan and vanillin-CMC coating solutions at all concentrations exhibited the inhibitory effect rather than those without vanillin. These results may be associated with an increase in fungal inhibitory mechanisms and are in agreement of previous researches, demonstrating that vanillin can also inhibit various microorganism growth, *i.e.*, bacteria, yeasts, and mold (López-Malo et al., 1995; Cerrutti & Alzamora, 1996; Fitzgerald et al., 2004). Fitzgerald et al. (2004) reported that vanillin has negative effects to bacteria's cell membrane, because of it causes a rapid release in K^+ to the outer bacterial cell, followed by changing of the pH homeostasis and resulted in bacterial lysis and death. The molecular structure of vanillin may be contributed to its antibacterial activity. It is consisted of two important functional groups including aldehyde and hydroxyl groups. The experiment of Chang, Chen, & Chang (2001) demonstrated that functional groups of natural antibacterial agents have influenced its antibacterial activity. The cinnamaldehyde gave greater antimicrobial activities against a range of bacterial strains than all of cinnamic acid, cinnamyl alcohol, or cinnamyl acetate. In the similar way, Fitzgerald et al. (2005) reported that its aldehyde group exhibited a key role in antifungal activity. Because of the aldehyde group is very reactive and can form covalent bonds with DNA and proteins (Feron et al., 1991). For the hydroxyl group of vanillin, it can also be donated the hydrogen ion, however, its role has less than aldehyde group (Fitzgerald et al., 2005). Consequently, coating solutions containing vanillin exhibited the better inhibition efficacy than both of chitosan and CMC alone.

From the results, the inhibitory effect between each active coating solution should be also compared. As shown in Table 4.3, indicated that PIRGs of vanillin-chitosan coating solutions comparing in the same concentration of vanillin were significantly higher than which of vanillin-CMC coating solutions ($p \leq 0.05$). Vanillin-chitosan coating solutions have various antifungal mechanisms more than the vanillin-CMC coating solution, including reactive functional groups by itself and of vanillin, resulting in they provides the greater inhibitory effect against mycelial growth of mango anthracnose fungi.

2) Inhibitory effects of active coating solutions against conidiospore germinations of mango anthracnose fungi

In this experiment, the inhibitory effect of active coating solutions on germination of *C. gloeosporioides*'s conidiospores was investigated by the slide culture technique. Spore suspensions tested with different coating solutions were cultured on PDA medium under a room temperature (25 ± 2 °C) for 6 h, before they were stained with a bromophenol blue (Sigma-Aldrich, Singapore) and observed under a light microscope with 400× magnificent. The parallel test were done and observed at 24 h under a light microscope with 400× magnificent. The experimental results obtained were shown in Figure 4.8 to 4.9. In the control (no coating solution), conidiospores of anthracnose fungi could be greatly germinated and normally formed germ tubes at 6 h. In the chitosan coating solution, conidiospores of anthracnose fungi could not be germinated at 6 h (Figure 4.8 A), but their germ tubes could be germinated after 24 h (Figure 4.9 B). Interestingly, the germination of conidiospore was absolutely inhibited and germ tubes were not observed at 6 h and 24 h in all vanillin-chitosan coating solutions. On the other hand, conidiospores in CMC treatment could be normally germinated at both 6 h and 24 h, which were similar to the control (Figure 4.9). Interestingly, there were no germ tubes formed in all vanillin-CMC coating solution treatments.

Previously, the inhibition of spore germinations by chitosan have been reported by several researches (Ghaouth, Ponnampalam, Castaigne, & Arul, 1992; Plascencia-Jatomea, Viniegra, Olayo, Castillo-Ortega, & Shirai, 2003; Xu et al., 2007; Meng, Yang, Kennedy, & Tian, 2010). The mechanism of the inhibition of fungal spore germination occurs through a direct interaction of chitosan on the spore cell wall. This interaction has been reported by Plascencia-Jatomea et al. (2003), the authors have verified the germination of spore in a media added with chitosan under a scanning electron microscope. The result found that spores of *Aspergillus niger* were coated with chitosan and bound to other spores, causing spore aggregation and morphological deformation such as echinulate spores. However, although mechanism of CMC to inhibit the fungal spore germination is not clear and still has not found any report, but it is possibly to form a direct interaction on the spore cell wall as similar as chitosan. Moreover, a combination of chitosan and vanillin may be contributed to the inhibition of fungal spore germinations, indicating the synergistic effect of both active substances. This synergistic effect caused the increase in inhibitory effects

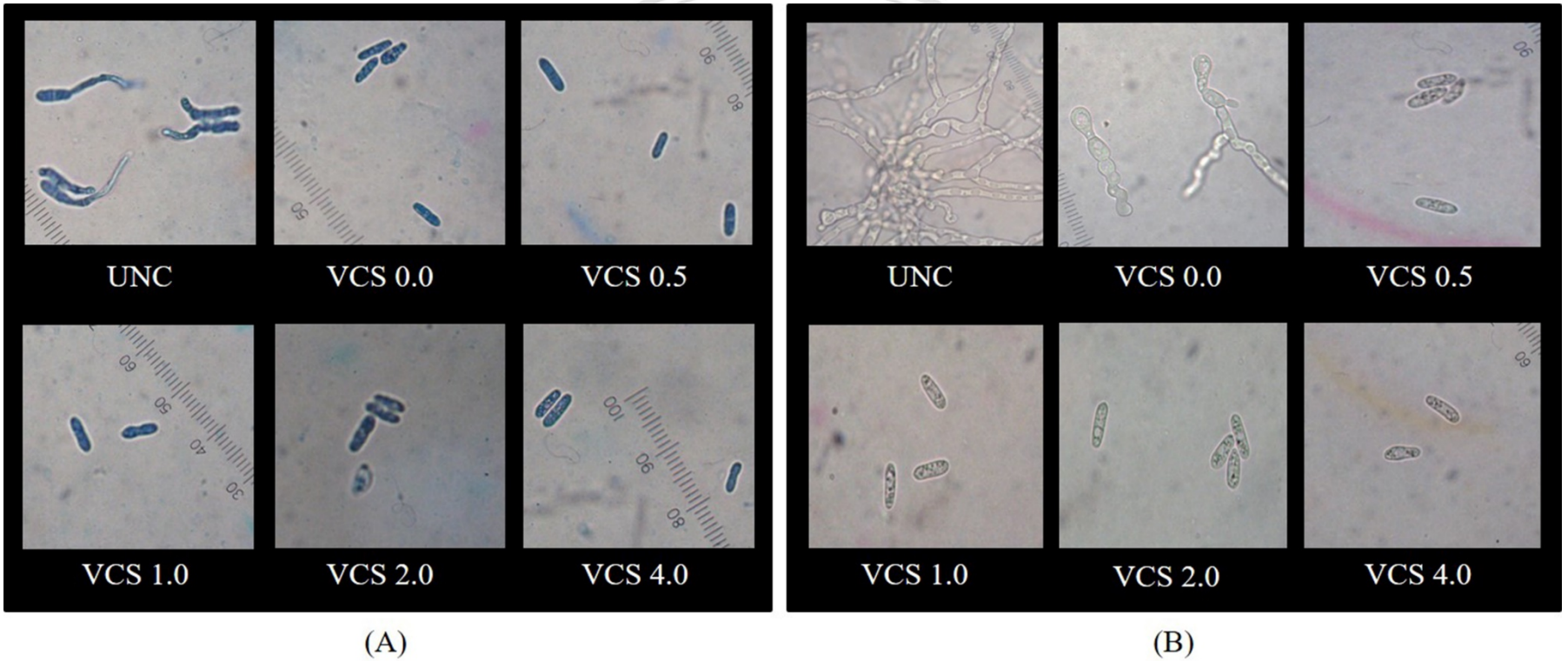

Figure 4.8 Antifungal effects of vanillin-chitosan coated paper against the conidiospore germination of *Colletotrichum* spp. cultured on the slide at 25 ºC for 6 h (a) and 24 h (b) under a light microscope at 400× magnification. Control and VCS 0.0 represent spore suspension alone and chitosan coating solution, respectively. VCS 0.5 to 4.0 define vanillin-chitosan coating solutions containing 0.5 to 4.0 % (w/v) of vanillin, respectively.

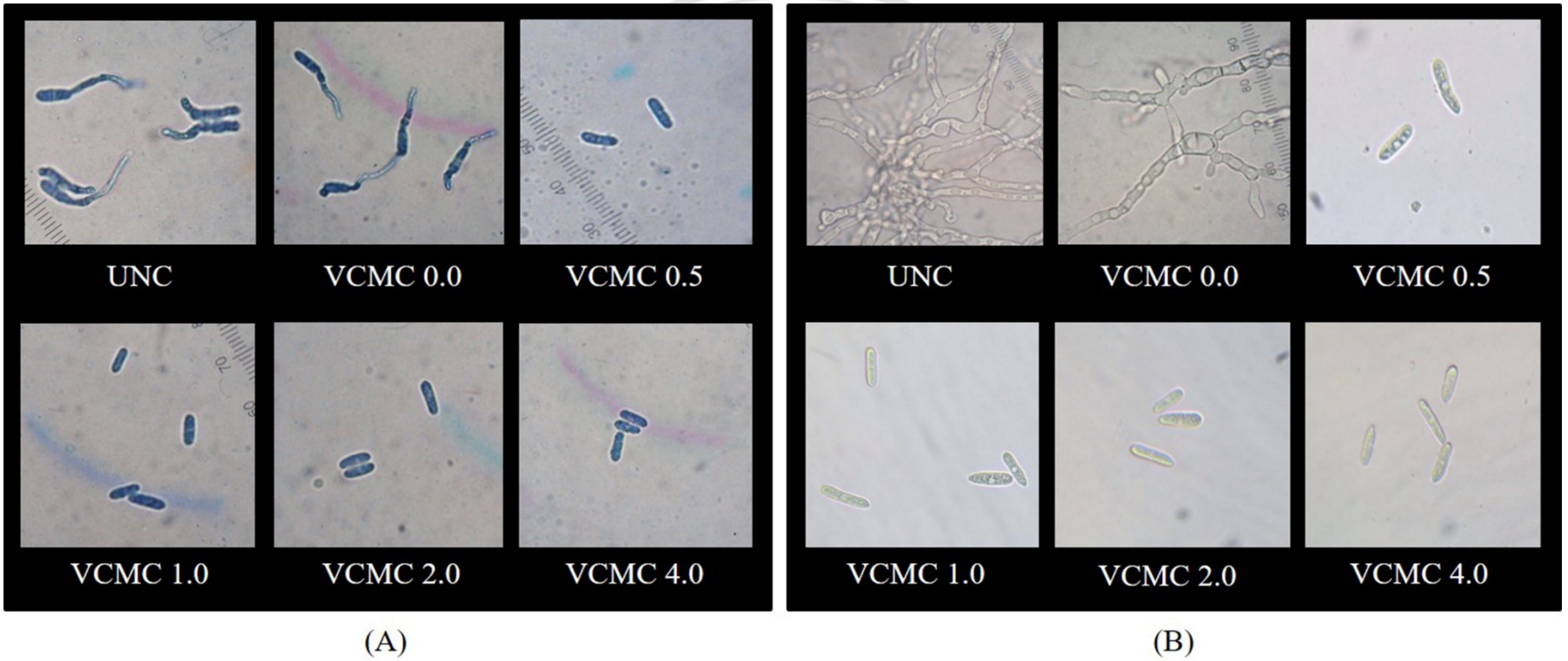

Figure 4.9 Antifungal effects of vanillin-CMC coated paper against the conidiospore germination of *Colletotrichum* spp. cultured on the slide at 25 ºC for 6 h (a) and 24 h (b) under a light microscope at 400× magnification. Control and VCMC 0.0 represent spore suspension alone and CMC coating solution, respectively. VCMC 0.5 to 4.0 define vanillin-CMC coating solutions containing 0.5 to 4.0 % (w/v) of vanillin, respectively.

against spore germinations of *C. gloeosporioides*. This is in agreement of Rahman et al. (2014), the authors found that the combination of chitosan and fungicide enhanced the inhibition of conidia germination of *Botrytis cinerea*.

4.2.3 Efficacy of Active-Coated Papers against Mango Anthracnose Fungi Evaluated by the Dual Culture Technique

1) Inhibitory effects of active-coated papers against mycelial growths of mango anthracnose fungi

In this experiment, the greater antifungal effect is considered from a smaller border size of radial mycelial growth of *Colletotrichum* spp. isolated from the infected mango fruit. As shown in Figure 4.10, anthracnose fungi had fully grown and spread over the UNC, indicating that paper had no antifungal effect. Similarly with the UNC, the VCMC 0.0 could not inhibit the mycelial growth of anthracnose fungi, while the VCS 0.0 could slightly inhibit the mycelial growth by considering from the smaller border size. According to the PIRG values that were summarized in Table 4.4, it showed that the antifungal effect of VCS 0.0 had only 5.83 % PIRG, while PIRG values of UNC and VCMC 0.0 were zero. Among three coated papers, the VCS 0.0 showed the strongest antifungal effect. This result might be attributed to protonated groups (NH_3^+) of chitosan that were formed under a hygroscopic condition and could electrostatically be interacted with negatively-charged fungal cell membrane components, such as proteins and phospholipids, leading to the leakage of intracellular components (Bautista-Banos et al., 2006). However, this interaction was not found in the coated papers of both UNC and VCMC 0.0.

For the effect of vanillin concentration, the result found that the stronger antifungal effect could be obviously seen in all of the vanillin-coated papers that provided the smaller border size of fungal mycelium than UNC, although the increasing of vanillin concentration had not related to the decreasing of mycelial size (Figure 4.10). In this case, the antifungal effect of both vanillin-chitosan and vanillin-CMC coated papers was significantly enhanced by increasing the concentrations of vanillin in the range of 0 to 1 % (w/v) ($p \leq 0.05$), as seen in Table 4.4, while the vanillin concentration more than this range had significantly lower antifungal effects ($p \leq 0.05$). At a given vanillin concentration, chitosan-coated papers gave the higher PIRG values than CMC-coated papers ($p \leq 0.05$) (Table 4.4).

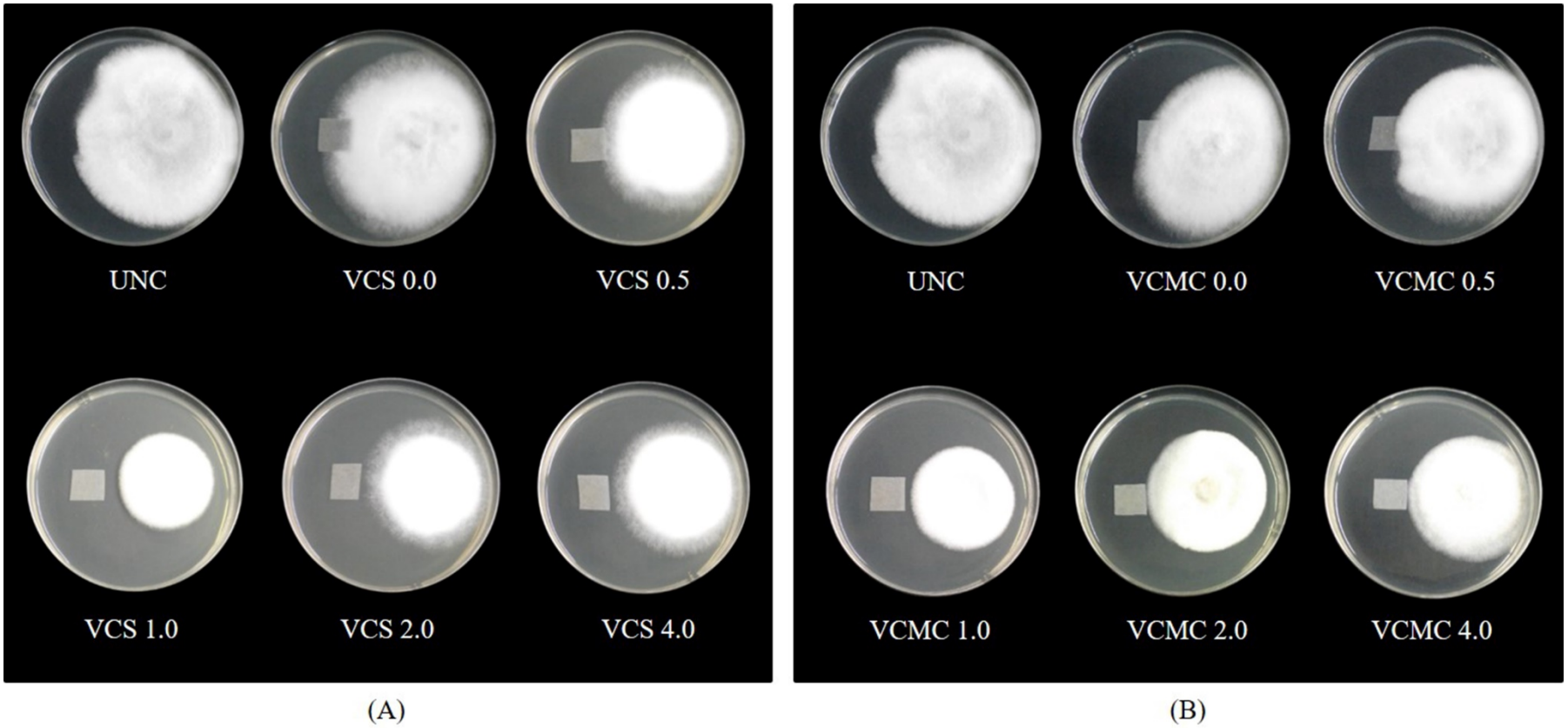

Figure 4.10 Antifungal effects of vanillin-chitosan coated paper (A) and vanillin-CMC coated paper (B) against the mycelial growth of *Colletotrichum* spp. on PDA at 25 ºC for 7 days. UNC, VCS 0.0, and VCMC 0.0 represent uncoated paper, chitosan-coated paper, and CMC-coated paper, respectively. VCS 0.5 to 4.0 define vanillin-chitosan coated papers containing 0.5 to 4.0 % (w/v) of vanillin, respectively. VCMC 0.5 to 4.0 define vanillin-CMC coated papers containing 0.5 to 4.0 % (w/v) of vanillin, respectively.

Table 4.4 The PIRG of *C. gloeosporioides* cultured on PDA for 7 days evaluated by the dual culture technique.

Treatments	PIRG (%)	Treatments	PIRG (%)
UNC	0.00 ^{ce} ± 0.00		
VCS 0.0	05.83 ^{eA} ± 0.42	VCMC 0.0	0.00 ^{ceB} ± 0.00
VCS 0.5	34.17 ^{dA} ± 0.39	VCMC 0.5	27.33 ^{cdB} ± 0.37
VCS 1.0	63.33 ^{aA} ± 0.33	VCMC 1.0	53.42 ^{caB} ± 0.39
VCS 2.0	43.33 ^{cA} ± 0.44	VCMC 2.0	35.75 ^{cbB} ± 0.42
VCS 4.0	49.17 ^{bA} ± 0.33	VCMC 4.0	39.00 ^{bcB} ± 0.33

Data shows the average ± standard deviation for investigating in three replications (n = 3).
Different lower case superscript letters in each column indicate significantly different at $p \leq 0.05$.
Different upper case superscript letters in each row indicate significantly different at $p \leq 0.05$.

The highest antifungal effect accompanied with the smallest border size of fungal mycelium were observed in VCS 1.0 (63.33 % PIRG) and VCMC 1.0 (53.42 % PIRG) ($p > 0.05$). The experimental results indicated that the stronger antifungal effect of the chitosan-coated paper incorporating with various vanillin concentrations might be attributed to the synergistic effect between chitosan and vanillin, while the antifungal effect of CMC-coated paper incorporating with various vanillin concentrations was dependent on the vanillin release because CMC did not show the antifungal effect. The reactive function group of vanillin can be directly damaged on cell membranes of the fungus causing cell lysis and eventually death (Feron et al., 1991; Papineau et al., 1991; Fitzgerald et al., 2005). Antifungal effects of vanillin-coated papers were depended on the concentration of vanillin. The highest PIRG of each vanillin-coated paper was found at only 1.0 % (w/v) of vanillin concentration. Due to the solubility of vanillin in water was 1 g/100 mL at 25 °C, the vanillin exceeding 1.0 % (w/v) in both chitosan and CMC coating solutions were re-crystallized at room temperature although it was completely soluble during preparation of coating solution (~83 °C). Thus, the vanillin concentrations exceeding 1.0 % (w/v) had lower PIRG values and was not suggested. In addition, antifungal effect of vanillin-coated papers was associated with release profile of active substance, which is vanillin. Vanillin was gradually

released and diffused through coating layers by the process of swelling, depending on its concentration. Stroescu, Stoica-Guzun, and Jipa (2013) demonstrated that the diffusion coefficient of vanillin decreased by increasing the concentration. Films containing lower vanillin concentrations absorbed more water, leading to greater swelling film layers as well. In greater swelling film layers, vanillin would be facilitated to easily diffuse out of the film.

2) Inhibitory effects of active-coated papers against conidiospore germination of anthracnose fungi

In this study, the effect of vanillin-coated papers against conidiospore germination of *Colletotrichum* spp. was examined by the slide culture technique. Conidiospore suspensions tested with all of the vanillin-coated papers were cultured on PDA at 25 °C for 6 h, before they were stained with a bromophenol blue and observed under a light microscope. Experimental results are shown in Figure 4.11, it was observed that the germ tube of conidiospore could normally germinated in the uncoated papers (UNC). Similarly to the UNC, the germ tube of anthracnose fungi in VCS 0.0 and VCMC 0.0 could also germinate after 6 h of testing. However, the conidiospore germinations were absolutely inhibited in all of the vanillin-coated papers and germ tubes disappeared. Both chitosan and CMC could not delay the germination of conidiospore through a direct interaction on conidiospore cell wall. For the chitosan, the fungal conidiospore spread onto the surface of chitosan film layers that was coated on the paper surface. Thus, one side of conidiospore cell wall was fixed by the protonated forms of chitosan through an electrostatic interaction and ultimately inhibited the germination of conidiospore whereas the CMC film layers on the coated paper did not have negative effects on fungal conidiospores. However, this study demonstrated that vanillin in coating solution could inhibit the germination of conidiospore. This result is attributed to the synergistic effects between chitosan or CMC and vanillin. Swelling structures of both chitosan and CMC film layers causes release of vanillin to fungal conidiospores and leads to expression of antifungal mechanisms.

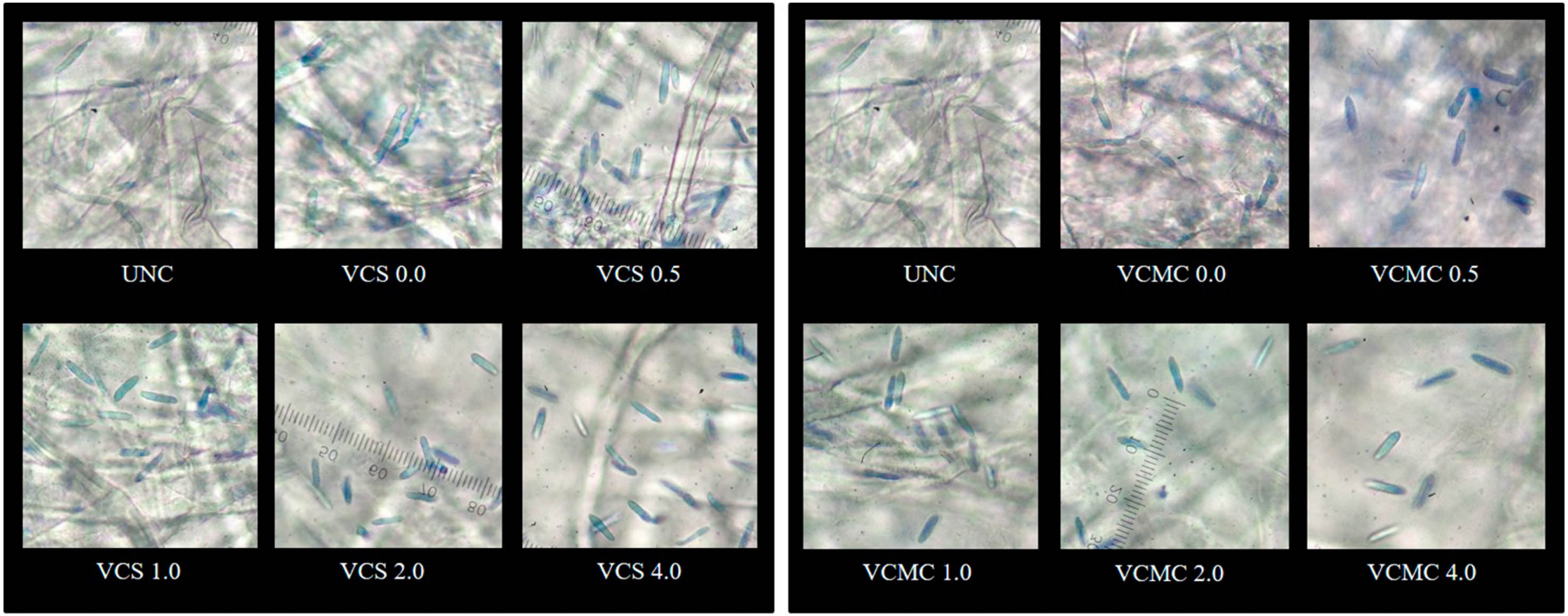

Figure 4.11 Antifungal effects of active wrapping papers including vanillin-chitosan coated paper (A) and vanillin-CMC coated paper (B) against the conidiospore germination of *Colletotrichum* spp. cultured on the slide at 25 ºC for 6 h under a light microscope at 400× magnification. UNC, VCS 0.0, and VCMC 0.0 represent uncoated paper, chitosan-coated paper, and CMC-coated paper, respectively. VCS 0.5 to 4.0 define vanillin-chitosan coated papers containing 0.5 to 4.0 % (w/v) of vanillin, respectively. VCMC 0.5 to 4.0 define vanillin-CMC coated papers containing 0.5 to 4.0 % (w/v) of vanillin, respectively.

4.2.4 Efficacy of Active-Coated Papers against Mango Anthracnose Fungi Evaluated by the Vapor-Diffusion Technique

In this experiment, the greater antifungal effect is considered from a smaller border size of radial mycelial growth of *Colletotrichum* spp. isolated from the infected mango fruit. Anthracnose fungi had fully grown and spread over all the treatments, indicating that there was low antifungal effects found in this experiment. There was no significant difference between the coated papers prepared from chitosan and CMC ($p > 0.05$). The experimental results indicated that increasing the vanillin concentrations also enhanced the percent inhibition of radial growth (PIRG) value ($p \leq 0.05$), as seen in Table 4.5. This result might be attributed to the larger concentrations of vanillin increased the volatile-vanillin fraction of active-coated papers. Thus, active-coated papers with higher concentration of vanillin could be greater inhibited the mycelial growth of anthracnose fungi and resulting in the greater PIRG values.

Table 4.5 The PIRG of *C. gloeosporioides* cultured on PDA for 7 days evaluated by the vapor diffusion technique.

Treatments	PIRG (%)	Treatments	PIRG (%)
VCS 0.0	$0.08^{dA} \pm 0.12$	VCMC 0.0	$00.04^{dA} \pm 0.06$
VCS 0.5	$3.83^{cA} \pm 0.12$	VCMC 0.5	$3.67^{cA} \pm 0.24$
VCS 1.0	$4.63^{cA} \pm 0.29$	VCMC 1.0	$4.46^{cA} \pm 0.29$
VCS 2.0	$6.67^{bA} \pm 0.59$	VCMC 2.0	$6.33^{bA} \pm 0.59$
VCS 4.0	$11.08^{aA} \pm 0.24$	VCMC 4.0	$10.83^{aA} \pm 0.24$

Data shows the average ± standard deviation for investigating in three replications ($n = 3$).
Different lower case superscript letters in each column indicate significantly different at $p \leq 0.05$.
Different upper case superscript letters in each row indicate significantly different at $p \leq 0.05$.

4.3 Efficacy of Active-Coated Papers on Ethylene Removal

Chitosan containing vanillin at 1 % (w/v), which gave the highest PIRG against *C. gloeosporioides* and the best inhibition conidiospore germination, was mixed with various types of ethylene adsorbents including zeolite (ZE) and activated carbon (AC) at various concentration (0.1, 0.2 and 0.4 %, w/v)). The capacity of ethylene adsorption of each treatment was monitored during storage for 35 days. Experimental results are shown in Table 4.6. It was found that all the ethylene adsorbent-coated papers could reduce the ethylene concentration during storage greater compared with both uncoated and vanillin coated papers ($p \leq 0.05$). Both zeolite and activated carbon exhibited the strongest effect for ethylene removal at 0.4 % (w/v). Additionally, it was found that the coated papers incorporating with zeolite could remove ethylene greater than those coated with activated carbon ($p \leq 0.05$).

The potential ethylene removal of zeolite associated with its surface area and reactive group. Moreover, the kinetic diameter of ethylene equal to 3.9 Å that fits to the pore opening of natural zeolite (approximately 4.0 to 7.2 Å) (Erdoğan, Sakızcı, & Yörükoğulları, 2008), whereas ethylene can easier move through the larger pore opening of activated carbon, resulting in its ethylene-entrapping efficacy is lower due to dispersion of ethylene. Ethylene could be adsorbed within the zeolite framework by two intermolecular interactions including cation···π and C–H···O interactions. The surface of zeolite contains abundant oxygen atoms as adsorption site, which can form the C–H···O interaction between C–H groups of ethylene and electronegative O of zeolite (Patdhanagul et al., 2010; Sue-aok et al., 2010). Likewise, it is also possible to form the cation···π interaction between the ethylene's π-orbital and the cation within the zeolite framework. However, both cation···π and C–H···O interactions are only a weak hydrogen bond and can be reversible. Additionally, the result also showed that the effect on ethylene removal of vanillin paper with either 0.2 or 0.4 % (w/v) zeolite (ZE 0.2 and ZE 0.4) was not different. Therefore, the vanillin paper incorporating 0.2 % (w/v) zeolite was the most suitable formula for preparing active-coated papers and used this concentration in the further study. From now, paper coated by chitosan-vanillin incorporated 0.2 % (w/v) zeolite will be called as zeolite paper (ZE 0.2).

Table 4.6 Changes of ethylene concentrations (ppm) during storage

Treatments	Storage times (Days)							
	0 ^{ns}	1	3	7	14	21	28	35
UNC	3.93 ± 0.03	3.77 ± 0.06 ^{a}	3.54 ± 0.04 ^{a}	3.36 ± 0.02 ^{a}	3.22 ± 0.02 ^{a}	3.21 ± 0.02 ^{a}	3.21 ± 0.02 ^{a}	3.20 ± 0.02 ^{a}
VCS 1.0	3.93 ± 0.06	3.64 ± 0.02 ^{b}	3.42 ± 0.02 ^{b}	3.24 ± 0.03 ^{b}	3.13 ± 0.02 ^{b}	3.12 ± 0.02 ^{b}	3.11 ± 0.03 ^{b}	3.10 ± 0.03 ^{b}
ZE 0.1	3.84 ± 0.09	3.26 ± 0.05 ^{ef}	2.83 ± 0.05 ^{e}	2.53 ± 0.05 ^{e}	2.28 ± 0.01 ^{e}	2.26 ± 0.01 ^{e}	2.24 ± 0.02 ^{e}	2.23 ± 0.02 ^{e}
ZE 0.2	3.87 ± 0.07	3.19 ± 0.04 ^{f}	2.55 ± 0.05 ^{f}	2.24 ± 0.02 ^{f}	2.01 ± 0.02 ^{f}	1.99 ± 0.02 ^{f}	1.98 ± 0.02 ^{f}	1.97 ± 0.02 ^{f}
ZE 0.4	3.83 ± 0.07	3.11 ± 0.02 ^{g}	2.47 ± 0.05 ^{g}	2.12 ± 0.04 ^{g}	1.95 ± 0.04 ^{f}	1.93 ± 0.05 ^{f}	1.91 ± 0.05 ^{f}	1.90 ± 0.05 ^{f}
AC 0.1	3.88 ± 0.08	3.56 ± 0.03 ^{c}	3.30 ± 0.03 ^{c}	2.97 ± 0.07 ^{c}	2.69 ± 0.04 ^{c}	2.67 ± 0.04 ^{c}	2.66 ± 0.04 ^{c}	2.65 ± 0.04 ^{c}
AC 0.2	3.83 ± 0.09	3.45 ± 0.05 ^{d}	3.15 ± 0.04 ^{d}	2.81 ± 0.08 ^{d}	2.56 ± 0.06 ^{d}	2.54 ± 0.06 ^{d}	2.52 ± 0.07 ^{d}	2.51 ± 0.06 ^{d}
AC 0.4	3.87 ± 0.09	3.33 ± 0.05 ^{e}	2.91 ± 0.05 ^{e}	2.62 ± 0.07 ^{e}	2.34 ± 0.03 ^{e}	2.32 ± 0.03 ^{e}	2.31 ± 0.04 ^{e}	2.30 ± 0.04 ^{e}

Different superscript letters in each column indicate significantly different at $p \leq 0.05$.

The superscript letter, ns, indicating that each column has not significantly different at $p > 0.05$.

4.4 Application of Active-Coated Papers by Wrapping on Mango Fruits

4.4.1 Properties of Active-Coated Papers for Wrapping Mango Fruits

In the previous experiment, ZE 0.2 was active-coated paper that was the most effective in adsorbing ethylene. It was prepared from VCS 1.0 that gave the highest PIRG (63.33 %) against the mycelial growth of *C. gloeosporioides*, as the causal fungi of anthracnose disease in mango fruits (Sangchote, 1987). Therefore, to investigate the effect of wrapping a mango fruit using an active-coated paper on the disease incidence and physi-cochemical properties of mango fruits, both VCS 1.0 and ZE 0.2 were selected to apply as an active-coated paper, comparing with a negative control (unwrapped mango fruits) and a positive control (mango fruits wrapped with UNC). Properties of active-coated papers are shown in Table 4.7.

Table 4.7 Properties of active-coated papers applied for wrapping mango fruits

Paper properties	Types of wrapping papers		
	UNC	VCS 1.0	ZE 0.2
Thickness (μm)	39 ^{b} ± 2	45 ^{a} ± 2	46 ^{a} ± 2
Moisture content (%)	6.25 ^{b} ± 0.37	7.61 ^{a} ± 0.12	7.71 ^{a} ± 0.23
*L**	87.74 ^{b} ± 0.24	87.28 ^{c} ± 0.08	88.11 ^{a} ± 0.22
*a**	0.38 ^{a} ± 0.02	-4.24 ^{b} ± 0.16	-4.10 ^{b} ± 0.17
*b**	5.61 ^{b} ± 0.20	19.79 ^{a} ± 0.19	19.69 ^{a} ± 0.06
WVP (× 10^{-4} g/ m^2.day Pa)	3.51 ^{a} ± 0.24	0.61 ^{b} ± 0.06	0.68 ^{b} ± 0.03
Tensile strength (MPa)	56.18 ^{b} ± 1.79	58.57 ^{a} ± 1.86	56.23 ^{b} ± 1.77
Elongation (%)	1.68 ^{c} ± 0.13	2.57 ^{a} ± 0.14	2.02 ^{b} ± 0.21

Data shows the average ± standard deviation for investigating three replications (n = 3).
Different superscript letters in each row indicate significantly different at $p \leq 0.05$.

The thickness and moisture content of VCS 1.0 were higher than UNC ($p \leq 0.05$). The addition of zeolite was not effect on the thickness and moisture content of VCS 1.0 and ZE 0.2 ($p > 0.05$), due to a homogeneous mixture between zeolite and vanillin-chitosan coating solution. Zeolite is crystalline, the framework is generally open and contains channels and cavities in which are located cations and water molecules (Breck, 1974; Dyer, 1988; Farrauto, 1997; Szostak, 1998). Therefore, its structure with containing amounts of water bound in their crystal grid (Marcus & Cormier, 1999), led to the slightly higher moisture content of coated papers containing zeolite. For the color properties, the coating could directly affect the brightness of coated paper, resulting in the VCS 1.0 had the lower L^* value than the UNC. Because of zeolite is a white mineral. The homogeneity of zeolite dispersion led to the significantly increased L^* value of ZE 0.2, which was significantly higher than both UNC and VCS 1.0 ($p \leq 0.05$). For the a^* and b^* value, the coating caused the change in a^* and b^* values. The a^* value of VCS 1.0 were lower than UNC ($p \leq 0.05$), but did not significantly different from ZE 0.2 ($p > 0.05$). Likewise, the b^* value of VCS 1.0 were also higher than UNC ($p \leq 0.05$), but did not significantly different from ZE 0.2 ($p > 0.05$). It might be due to the yellowness of vanillin.

The result exhibited that WVP value of the VCS 1.0 was significantly lower than the UNC ($p \leq 0.05$), while WVP values of VCS 1.0 and ZE 0.2 were not significantly different ($p > 0.05$). The chitosan film covered on the surface of VCS 1.0 and ZE 0.2 could resist the water vapor greater than the UNC without any coating layer, because of the UNC have a hydrophilic nature and contained a lot of porous surface. As previously mentioned, WVP is a property that is directly related to the hydrophilic nature of film, films with more hydro-philicity have the greater WVP (Tongdeesoontorn et al., 2009). Chitosan films are polysac-charide based film, tend to exhibit fat and oil resistance and selective permeability to gases but lack resistance to water transmission (Bordenave et al., 2007; Sebti, Martial-Gros, Carnet-Pantiez, Grelier, & Coma, 2006) due to strongly hydrophilic character, leading to an interaction with water molecules.

The results of tensile strength and elongation were shown in Table 4.7, which shown that the coating changed mechanical properties of the paper. Both tensile strength and elongation of the VCS 1.0 had significantly higher values than of the UNC ($p \leq 0.05$). However, the incorporation of zeolite reduced tensile strength and elongation of vanillin coated paper. The bulky structure of zeolite made the film loss of its segmental mobility.

Although it provides the desired ethylene absorber effect, it weakens the polymer structure. It was found that the tensile strength and percent elongation were decreased significantly when adding zeolite in coated paper. Chang, Akil, and Nasir (2013) reported that the addition of zeolite into ultra-high molecular weight polyethylene matrix reduced the tensile strength and elongation at break. Additionally, zeolite content, particle size, and heterogeneous structure of chitosan matrix with zeolite particle could affect the mechanical particle size on mechanical properties of epoxy systems. With increasing zeolite content, tensile strength and impact strength decreased. As the zeolite particle size decreased, all these properties increased. Characteristics of the paper surface under SEM are shown in Figure 4.12. The surface of UNC had a lot of porous, while VCS 1.0 papers had the smoother surface. For ZE 0.2, it was found a zeolite particle dispersed in chitosan matrix.

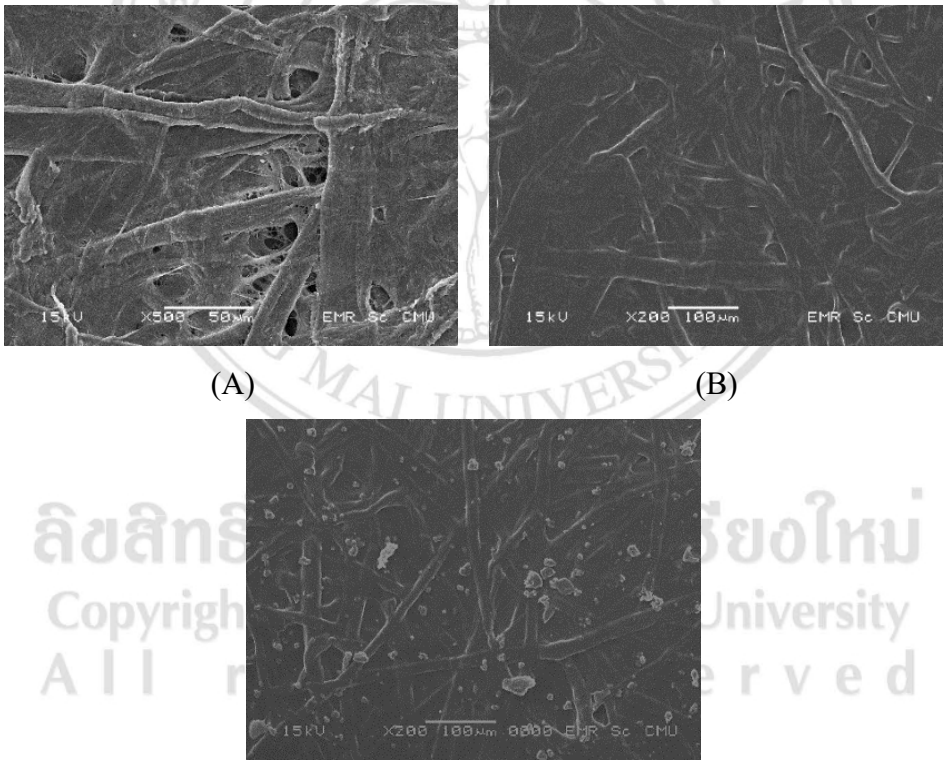

(A) (B)

(C)

Figure 4.12 Paper surface topography (200x); for uncoated paper (UNC) (A), chitosan-coated paper incorporating with 1 % vanillin (VCS 1.0) (B) and VCS 1.0 incorporating with 0.2 % zeolite (ZE 0.2) (C)

4.4.2 Disease Incidence on the Inoculated Mango Fruit

There were no incidence of anthracnose in the initial storage. On Day 10, the disease incidence was obviously shown in unwrapped fruits and fruits wrapped with UNC (Figure 4.13). The inoculated mango fruits appeared black circular spots on the peel of mango fruits with varying sizes. These black spots expanded and later became sunken and collapsed, forming larger spot (Sangchote, 1987). Interestingly, one third of mango fruits for both unwrapped fruits and fruits wrapped with UNC were also infected at stem end while no disease incidence appeared on fruits wrapped by VCS 1.0 and ZE 0.2. This result indicated that both VCS 1.0 and ZE 0.2 could inhibit anthracnose fungi in mango fruits better than unwrapped fruits and fruits wrapped by UNC during 10 days of storage. However, to confirm the antifungal effect of active-coated papers under the actual storage condition, the severity index of disease (SID) was also evaluated in the next experiment.

4.4.3 Severity Index of Anthracnose Disease on the Wrapped Mango Fruit

In this experiment, all mangoes were stored under 13 °C and 90 % RH to avoid the conidia germination and formation of appressorium. Mango fruits were checked every 3 days. The severity index of disease of the mango fruit wrapped with different wrapping papers was evaluated using the extent of total black spots on each fruit surface occurred from anthracnose diseases caused by *Colletotrichum* spp. Sometime a postharvest rot of mango fruit *cv* Nam Dok Mai have been reported that it is also caused by other kinds of fungi such as, *Aspergillus niger*, *Botryodiplodia theobromae*, *Dothiorella dominicana*, and *Phomopsis mangiferae* (Sangchote, 1987). Consequently, the symptom of all diseases that appeared on the surface of mango fruit was used for assessing the index disease in this study. The severity index of disease (SID value) could be calculated by Equation (4.2) (Zheng, Tian, Xu, & Li, 2005). Severity scales are classified as 5 groups described in Table 4.8.

$$\text{SID value} = \frac{\sum(\text{Severity scale} \times \text{Number of fruit in each group})}{\text{Number of total fruit} \times \text{Highest severity scale}} \times 100 \quad (4.2)$$

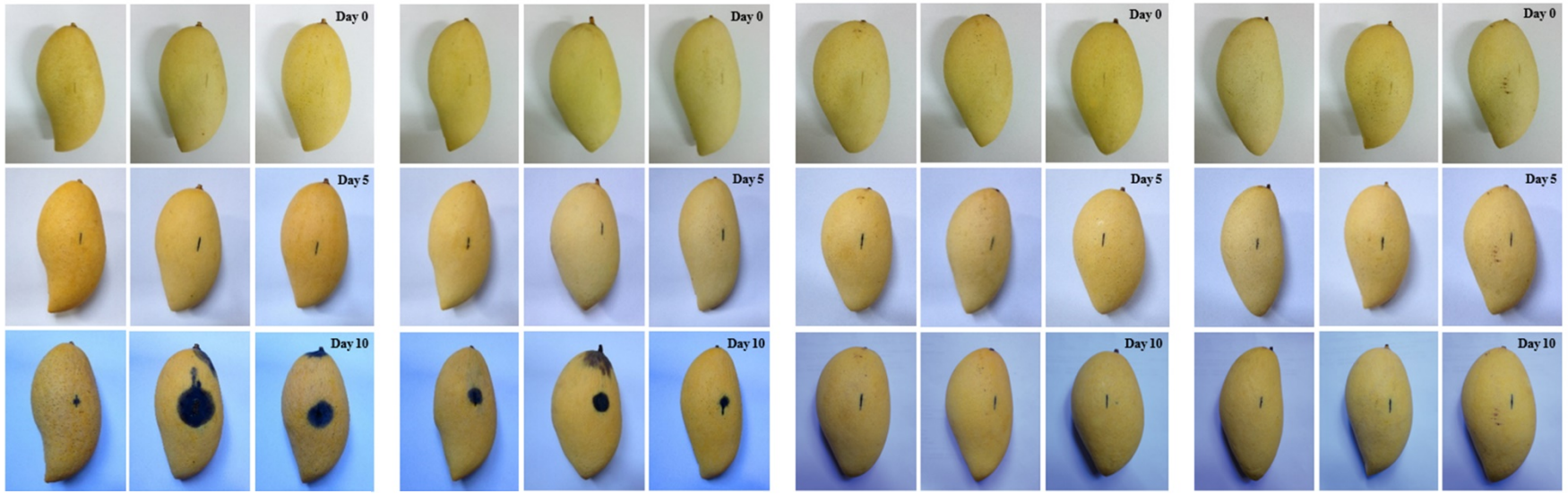

Figure 4.13 Disease incidences on the artificially-inoculated mango fruits during storage at 25 °C for 10 days; Unwrapped fruits (A), fruits wrapped with uncoated paper (UNC) (B), chitosan-coated paper incorporating with 1 % vanillin (VCS 1.0) (C) and VCS 1.0 incorporating with 0.2 % zeolite (ZE 0.2) (D).

Table 4.8 Disease index of mango fruits (Zheng et al., 2007)

Disease scale	0	1	2	3	4
Description	No visible decay	< 1 % decay	1 – 20 % decay	20 – 50 % decay	> 50 % decay
Sample					

As shown in Figure 4.14, there was no disease incidence in all treatments on Day 3. Later time SID values for all samples were continuously increased throughout the experimental period. The disease incidence of unwrapped fruit and the fruit wrapped with UNC were firstly observed on Day 6, while the fruits wrapped with VCS 1.0 and ZE 0.2 remained no disease incidence at this time. The first disease incidence of fruits wrapped with VCS 1.0 and ZE 0.2 were observed on Day 9 and Day 12 of storage, respectively. Fruits wrapped with ZE 0.2 had the obviously lowest SID value. On Day 30, the fruit wrapped by ZE 0.2 had the significantly lower SID value (56.67 %) than unwrapped fruit (85.83 %), the fruit wrapped by UNC (86.67 %) and VCS 1.0 (65.00 %) ($p \leq 0.05$). Therefore, ZE 0.2 was the most effective active-coated paper, which could inhibit the anthracnose disease causing a postharvest decay in mango fruits.

The inhibition effect of VCS 1.0 and ZE 0.2 could occur in 3 patterns. Firstly, direct contact between mango and coated layer, which had a positively-charged chitosan. Secondly, a vanillin which is a phenolic volatile compound in VCS 1.0 could be released from chitosan matrix to inhibit the growth of anthracnose fungi. The increase in surrounding RH caused by respiration led to swelling of the chitosan layers and eased the vanillin release. Diffusion of active compound can occur through chitosan matrix but will be more facilitated by the polymer swells in contact with water vapor (Kurek, Guinault, Voilley, Galic, & Debeaufort, 2014). In swelling-controlled systems, polymer which interacts with the penetrant undergoes a transition from a glassy to a rubbery state. The polymer chains in the rubbery state, being more mobile than in the glassy state, allow the active agent to diffuse out of the matrix more rapidly (Mastromatteo et al., 2010). Thirdly, a semi-volatile characteristic of vanillin in those papers can also diffuse across the headspace air to function on the surface of mango fruit.

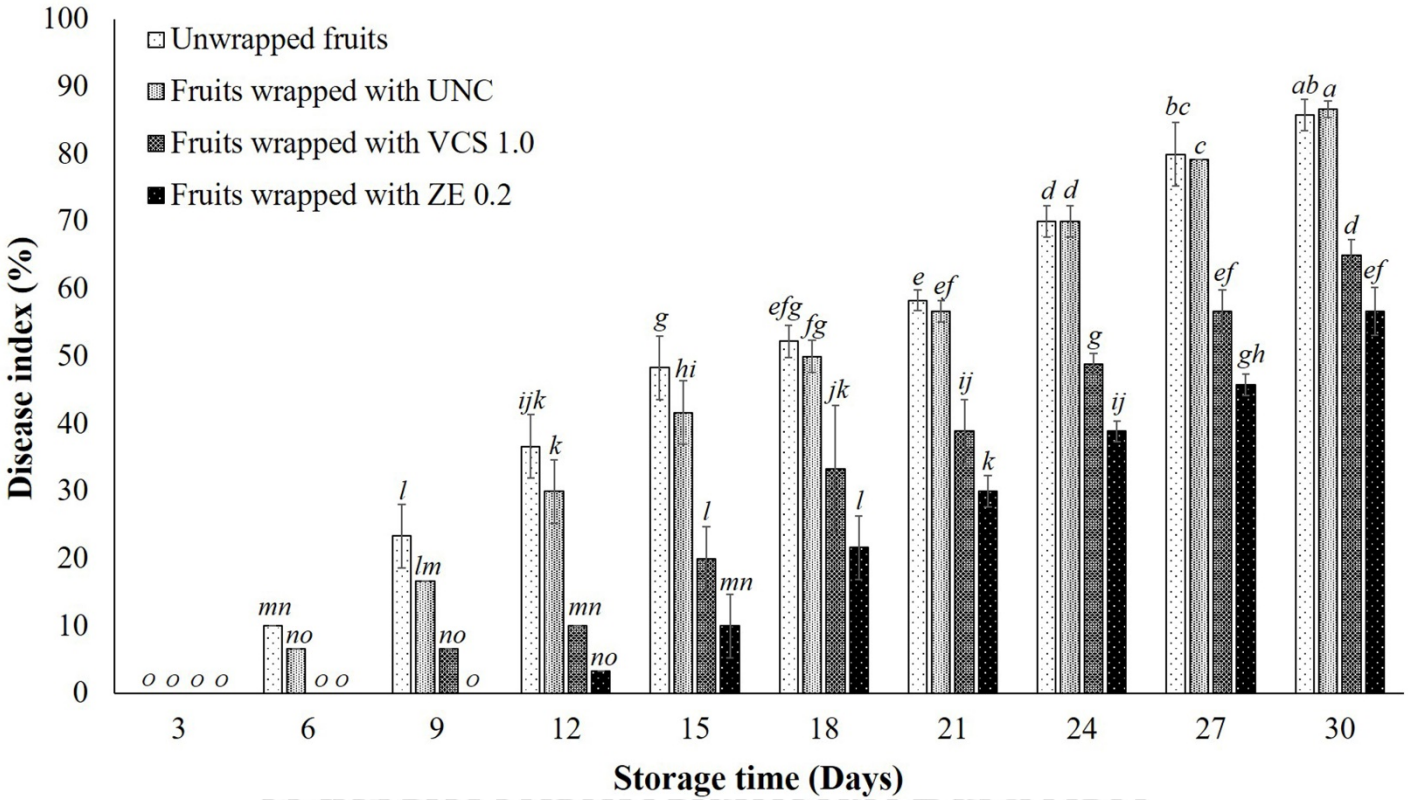

Figure 4.14 Severity index of anthracnose disease in mango fruits during storage under 13 °C and 90 % RH for 30 days. Data in each bar show the average ± standard deviation for evaluating 30 replications. Different letters indicate significant difference at $p \leq 0.05$.

About the implication of the inhibition of conidial germination, which is probably latent-infected since in the field. Here, conidia are rain-splashed to other leaves/ flowers, thus developing fruits can also be infected. However, infections remain quiescent until the onset of ripening which occurs after harvest (Arauz, 2000). A fungal quiescence in a climacteric fruit is terminated by the reduction of its antifungal compound and/or by the ethylene production during ripening (Flaishman & Kolattukudy, 1994; Prusky, 1996). During ripening of mango fruits, the fungal conidia began to germinate germ tubes and form appressoria. Afterwards, the hypha formed by the appressorium emerges at the pore and penetrates through the cuticle into the epidermis of fruit, causing mycelial growth.

The result reflected that both unwrapped fruits and fruits wrapped by UNC had no effect on the inhibition of conidial germination of anthracnose fungi because they could normally germinate on the surface of mango fruit since 6 days of storage. Moreover, the greater inhibitory effect was found in fruits wrapped by VCS 1.0 and the best was found in fruits wrapped by ZE 0.2 in which the germination of conidia was inhibited and delayed to Day 9 and Day 12 of storage, respectively. It was possible that several metabolic processes, stimulating by ethylene, such as respiration and transpiration, were slowed down due to the active-coated paper. The termination of fungal quiescence was delayed to Day 12. When the conidia of anthracnose fungi germinated, they developed a mycelium. The anthracnose incidence could obviously be seen and began to extend the damage border on the fruit surface (*i.e.*, black spot). ZE 0.2 is the most effective against anthracnose accompanied with the ethylene adsorption capacity during mango fruit ripening as well.

4.4.4 Physical Quality of Wrapped Mango Fruits

1) Weight loss

Weight loss is one of the important determinants of mango storage life. It is well-known that weight loss of climacteric fruits is attributed to the mechanisms of respiration and transpiration through the peel tissue, leading to weight loss, appearance (wilting and shriveling), textural quality (softening, flaccidity, limpness, crispness and juiciness), and nutritional quality. The antimicrobial effect of coated paper on the quality of postharvest fruits have previously been reported (Rodríguez, Batlle, & Nerín, 2007). However, changes in weight loss during storage for wrapped fruits has not been reported.

Weight loss data are shown in Figure 4.15. Increasing the storage time significantly enhanced the weight loss for all samples ($p \leq 0.05$). The similar trends have been also reported in other unwrapped climacteric fruits, *i.e.*, tomato, papaya and peach (Nunes & Emond, 2007). After storage for 30 days, mango fruits wrapped by ZE 0.2 and VCS 1.0 had no significantly different in weight loss but the weight loss of these treatments were significantly lower than that of UNC and unwrapped fruits ($p \leq 0.05$), in which their weight loss were 10.38, 10.56, 11.51, and 12.67 %, respectively. All treatments showed the lower weight loss than which of direct coating, which has been reported by Hoa, Ducamp, Lebrun, and Baldwin (2002). The authors studied the effect of direct coating on weight loss of mango fruits (Kent and Tommy Atkins from Israel, and Lirfa from Reunion Island) using several coating formulas, and found that weight loss was in the range of 15.0 to 20.9 % after 17 days of storage under 12 °C and 80 % RH, which was slightly different from this study (13 °C and 90 % RH).

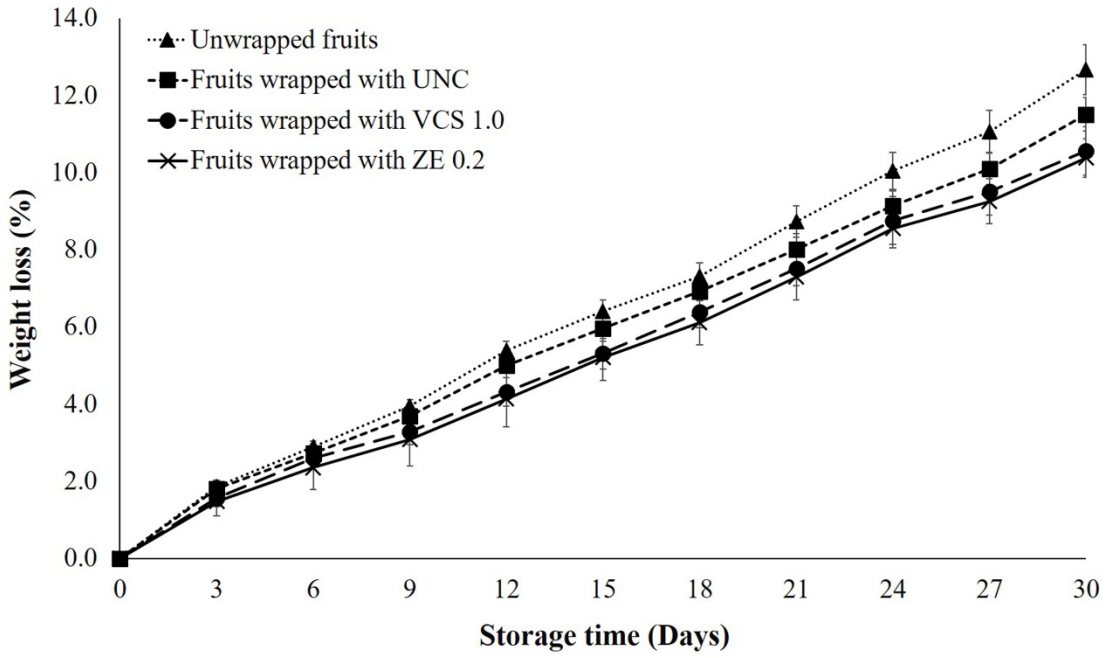

Figure 4.15 Changes in weight loss of mango fruits during storage at 13 °C for 30 days.

Under similar storage condition, the important reason for the reduction of weight loss may involve to respiration and transpiration, which are common metabolic processes occurring in living plant tissues as well as fruits. Three factors including temp-

erature, RH and air movement are the most significant factors affecting these processes. Storage of most fruits under a cool temperature (13 ± 2 °C), high atmospheric RH (90 ± 2 %) and low air movement is good for extending the shelf life. Under low temperature, metabolic processes are retarded. Likewise, under high atmospheric RH and low air movement, the mass transfer process of water vapor is reduced (Mishra & Gamage, 2007). These facts are the causes of increased weight loss during storage. The UNC might act a remarkable role as the water barrier against water loss from a transpiration while both VCS 1.0 and ZE 0.2 showed better performance, because of the surface porosity of both papers was covered by coating solutions.

To prove that coating solution can reduce water loss, the water vapor permeability (WVP) of wrapping paper was evaluated. WVP of VCS 1.0 and ZE 0.2 were determined using ASTM E96/E96M-16 and found that the WVP values of VCS 1.0 (0.61×10^{-4} g/m^2·day·Pa) and ZE 0.2 (0.68×10^{-4} g/m^2·day·Pa) were significantly lower than that of UNC (3.51×10^{-4} g/m^2·day·Pa) ($p \leq 0.05$). Lower WVP retarded water loss from environment surrounding mango fruit to outside. These also might be contributed to the movements of air and water vapor around the headspace were more limited, causing an accumulation of them in this region where they could not freely disperse to the outer atmosphere. The accumulation of CO_2 and water vapor slower transpiration rate. Thus, wrapped mango fruits exhibited the lower weight loss than unwrapped fruits, which had no any barrier to retard the transpiration rate.

Additionally, chitosan coating on the mango fruit surface was effective to reduce the loss of weight (Cissé, Polidori, Montet, Loiseau, & Ducamp-Collin, 2015; Jongsri, Wangsomboondee, Rojsitthisak, & Seraypheap, 2016). However, excessive coating on the surface of fruit has negative impacts because very thick coating layer becomes an undesirable barrier between the internal fruit and the outer atmosphere and restricts an exchange of respiratory gas (Cisneros-Zevallos & Krochta, 2003). Modification of the internal atmosphere by coating can enhance disorders in the respiratory metabolism, resulting in high CO_2 and low O_2 concentration such as accumulation of ethanol and alcoholic off-flavor (Dhall, 2013). Park, Chinnan, and Shewfelt (1994) also reported that direct coating with 66 μm (or 2.6 mm) of edible zein changed the internal atmosphere of coated tomato fruits due to low O_2 and high CO_2, and led to alcohol production. Extremely low O_2 contents for broccoli also resulted in off-flavors due to anaerobic metabolism

(Weichmann, 1987). Therefore, wrapping of mango fruit with permeable active-coated papers may be more suitable process to avoid sensory implication occurring from an anaerobic metabolism when using direct coating on mango fruit.

2) Firmness

Fruit firmness is a major attribute expressing a softening, crispness, and freshness of the mango fruit. A higher firmness value shows a lower fruit softening. According to the experimental results shown in Figure 4.16, increasing of storage time dramatically decreased the fruit firmness in all treatments. This similar trend was consistent with other climacteric unwrapped fruits and directly coated fruits (Yaman & Bayoundrlı, 2002; Patil & Shanmugasundaram, 2015). At the end of storage, all the wrapped fruits showed the firmness in ranges of 1.89 to 4.79 N which was significantly higher than unwrapped fruits (1.11 N) ($p \leq 0.05$). Mango fruits wrapped with ZE 0.2 showed the highest firmness, followed by VCS 1.0, UNC and unwrapped fruits. Firmness had inverse relationship with weight loss.

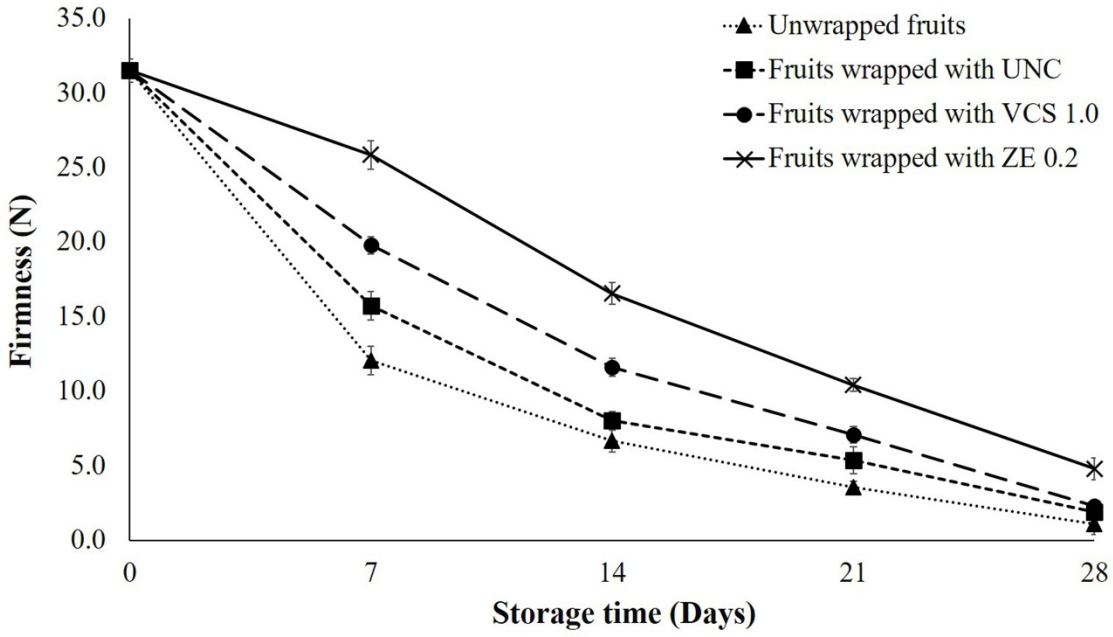

Figure 4.16 Changes in firmness of mango fruits during storage at 13 °C for 28 days.

The firmness of mango fruit decreased by increasing of storage time in all treatments, showing fruit softening process. The activities of pectolytic enzymes including β-galactosidase, pectin methylesterase and polygalacturonase are involved in decreasing of pectin molecular weight (Yashoda, Prabha, & Tharanathan, 2006) and soften mango fruits. Fruit softening is more accelerated by the formation of pathogen-infected lesions, which can induce the production of ethylene (Mattoo & Suttle, 1991). The increased concentration of ethylene triggers the respiration rate (Prasanna, Prabha, & Tharanathan, 2007) leading to increasing of enzymatic activities and faster fruit softening. ZE 0.2 helped to greatly preserve the firmness of mango fruit. Zeolite in ZE 0.2 acted as an ethylene absorber, which help removed the ethylene gas that activating the ripening process. When the ethylene gas was removed, the softening of mango fruit was delayed. Moreover, carbohydrate metabolisms in associated with a respiration to convert sugar and O_2 into respiratory by-products (water, CO_2, and energy) were also reduced. Likewise, vanillin in ZE 0.2 also acted as an antifungal agent, which could effectively inhibit anthracnose fungi. This result was correlated with anthracnose incidence which could obviously be seen in mango fruits with high SID value, especially the unwrapped fruits and fruits wrapped by UNC, which had very low firmness since 7 days of storage.

3) Color changes of mango fruits

Color is one of the important attributes directly affects the consumer acceptability in a fruit quality. Changes in the CIE LAB color space, L^* (lightness), a^* (redness), b^* (yellowness) values in unwrapped mango fruits and mango fruits wrapped by UNC, VCS 1.0, and ZE 0.2 during storage for 28 days were monitored. The results obtained are shown in Figure 4.17 to 4.19. The lightness of fruits had a tendency to continuously decrease throughout the experimental period in all treatments (Figure 4.17). Fruits wrapped by both VCS 1.0 and ZE 0.2 had slightly higher lightness than those wrapped by UNC and unwrapped fruits ($p > 0.05$). The damage expansion occurring from infected lesions might be a major cause leading to the lower lightness for the UNC than VCS 1.0 and ZE 0.2. VCS 1.0 and ZE 0.2 reduced the decay by the anthracnose infection on mango fruit, in which an infected lesion on fruits induced the production of ethylene leading to acceleration of the fruit ripening. Rather than the inhibition of disease, the zeolite in ZE 0.2 could also adsorb ethylene surrounding mango fruit. Therefore, the ripening process was delayed and thus the

change of L^* in VCS 1.0 and ZE 0.2 were delayed as well. On the other hand, the redness of mango fruits continuously increased throughout the experimental period (Figure 4.18). Mango fruits wrapped with ZE 0.2 showed the slower change in the redness value than which were wrapped by other papers and unwrapped fruits. ZE 0.2 provided a good barrier against the dispersion of respiratory gases accompanied with the ethylene adsorption capacity. It resulted in the lowering of ethylene and the increasing of CO_2 inside the headspace. Under the condition having the elevated CO_2 concentrations more than 1.0 % ripening of fruit was delayed resulted in slower degradation of chlorophyll pigment (Ahmad et al., 2001; Zapata et al., 2008). Changes in the yellowness of mango fruit is shown in Figure 4.19. The b^* value of unwrapped fruits rapidly increased in 7 days of storage until reached the peak, afterward, the b^* value dramatically decreased until the end of storage while b^* values of fruits wrapped by all the wrapping papers rapidly increased in 7 days with the slower rate than unwrapped fruits. The peak was reached on Day 14 and continuously decreased until the end of storage. The result reflected that the yellowness of fruits wrapped by all types of the papers were delayed. Mango fruits wrapped with the ZE 0.2 had the lower yellowness than other papers throughout the experimental period due to it had the best efficacy on the ethylene removal.

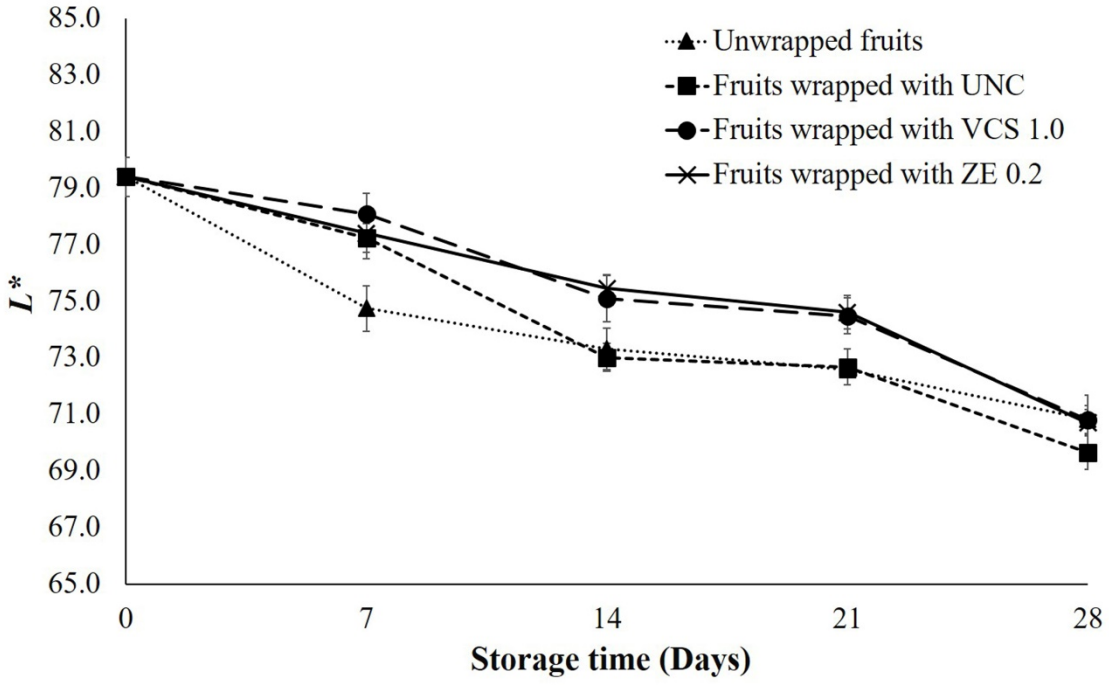

Figure 4.17 Changes in L^* value of mango fruits during storage at 13 °C for 28 days.

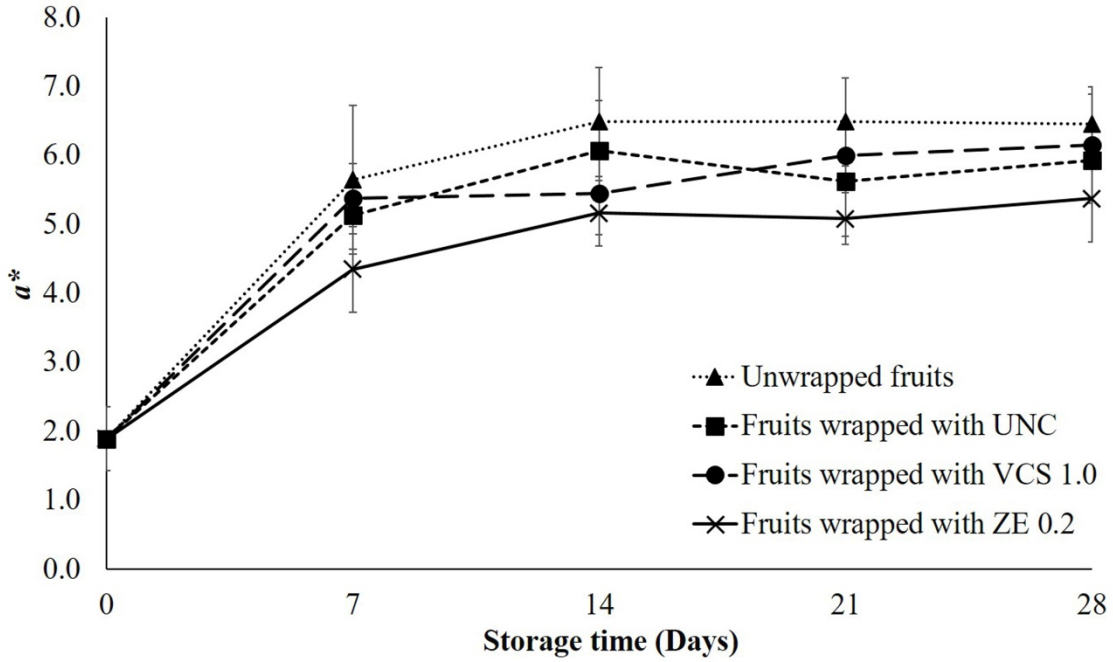

Figure 4.18 Changes in *a** value of mango fruits during storage at 13 °C for 28 days.

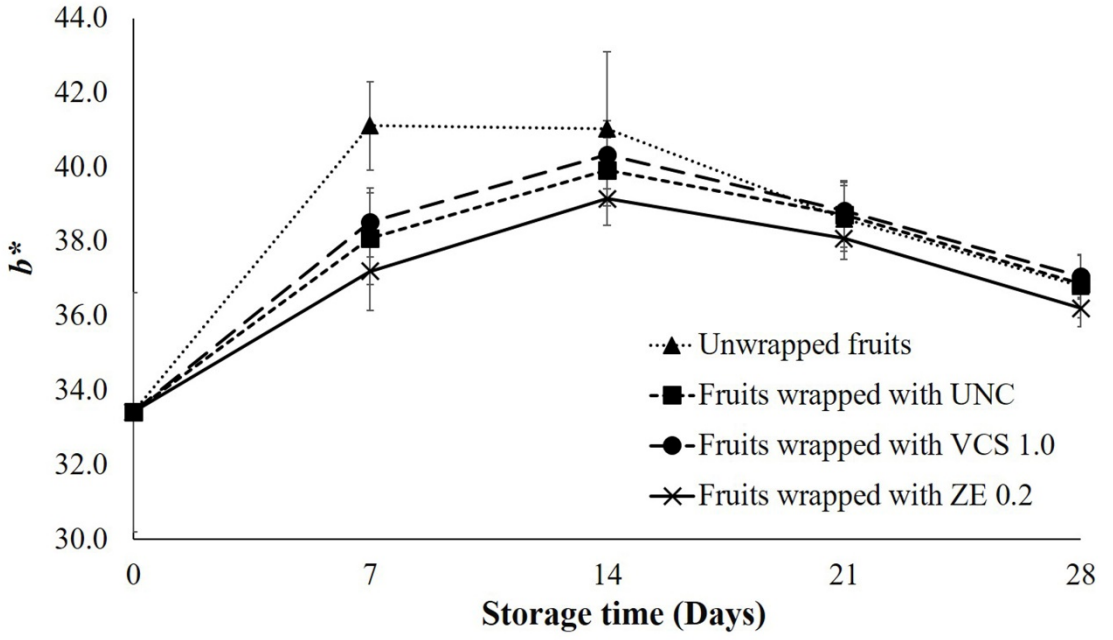

Figure 4.19 Changes in *b** value of mango fruits during storage at 13 °C for 28 days.

4.4.5 Chemical Quality of Wrapped Mango Fruits

1) Titratable acidity

Titratable acidity (TA) is an important indicator of fruit ripening which reflects the conversion of starch to organic acids used in fruit respiration. In this study, all treatments were sampled to analyze TA value using a titration method and expressed as percent of citric acid. The results are shown in Figure 4.20. At the initial storage time, TA of mango fruits was 3.25 %. As storage time passed, TA values decreased in all treatments. Similar trends have also been reported in other varieties of mango fruit (Kim et al., 2007; Rathore, Masud, Sammi, & Soomro, 2007). The reduction of TA values in all treatments might be due to organic acids (such as citric acid, malic acid) existing in mango fruits directly used in the citric acid cycle.

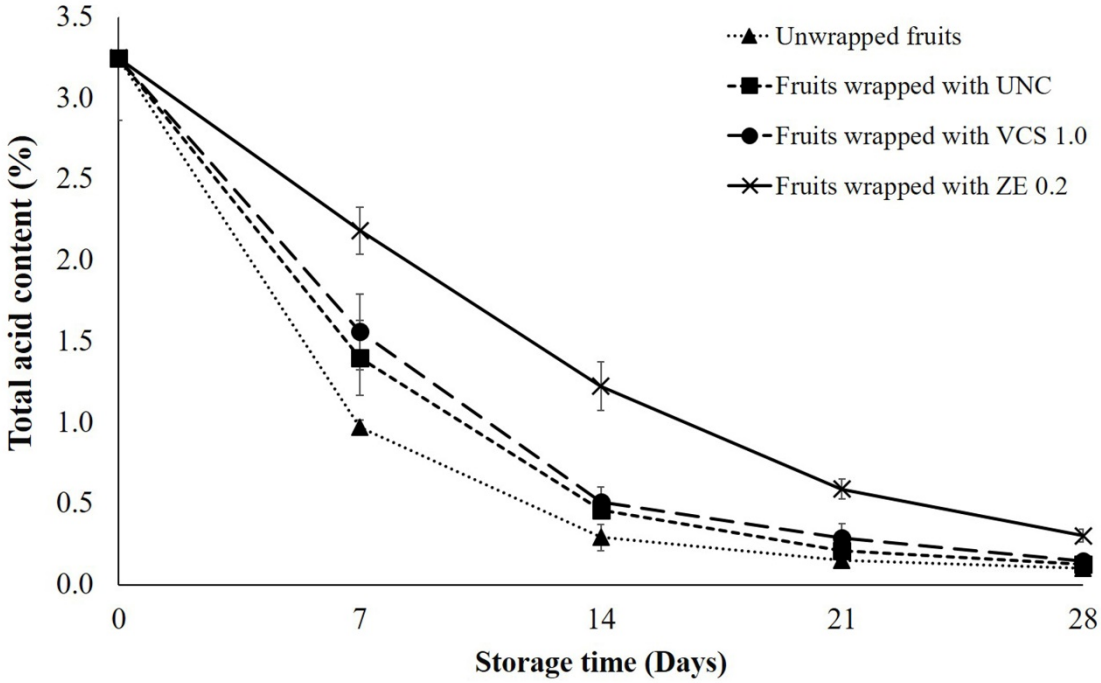

Figure 4.20 Changes in titratable acidity of mango fruits during storage at 13 °C for 28 days

At the end of storage, TA values of all treatments were in the range of 0.10 to 0.30 %. Fruits wrapped with zeolite paper exhibited significant highest TA value ($p \leq 0.05$) due to the efficacy of zeolite which slow down the ripening process accelerated

by accumulation of ethylene, causing delay in metabolic changes of fruits. This agreed with Garcia, Casariego, Diaz, and Roblejo (2014) who reported that tomatoes coated with chitosan/zeolite showed a slower decrease in TA than tomatoes coated with chitosan, chitosan/tween 80 and uncoated tomatoes during the storage period of 37 days at 10 ºC. However, differences with respect to coated samples were not significant. Additionally, although the VCS 1.0 could delay fruit ripening by inhibiting aerobic respiration of infected lesions, however, there was no difference with fruits wrapped by UNC ($p > 0.05$).

2) Total soluble solid

Total soluble solids (TSS) are used as an indicator of fruit maturity. It is defined as whole compositions of water-dissolved solids in juices including sugars (*i.e.*, sucrose, glucose, fructose), organic acids (*i.e.*, malic acid, citric acid), and free amino acids. TSS is determined by a refractrometer (Master, Atago, Japan) and expressed as the percentage. During fruit ripening, sugars are the major composition of soluble solid, particularly a ripe mango fruit, which has very high sugar content and can reach levels in excess of TSS (Paliyath & Murr, 2008). The sugar content in mango fruits is generally evaluated in the terms of TSS. As shown in Figure 4.21, the TSS of mango fruits was 12.50 % at an initial storage time. TSS in unwrapped fruits and fruits wrapped by UNC were enhanced and the highest peak on Day 14, and afterwards TSS decreased until the storage ended, whereas TSS in fruits wrapped by VCS 1.0 and ZE 0.2 were continuously increased to the peak on Day 21 before they slightly decrease. This evident confirmed that VCS 1.0 and ZE 0.2 can delay fruit ripening and thus extended storage life of wrapped mango. The similar trend is also reported by previous studies (Hoa et al., 2002; Rathore et al., 2007). At the end of storage, TSS of all fruits ranged from 15.67 to 18.53 %. Fruits wrapped by ZE 0.2 showed the highest TSS ($p \leq 0.05$), followed by VCS 1.0, UNC, and unwrapped fruits, which were 17.13, 16.47, and 15.67 %, respectively. Increasing of TSS during fruit ripening were normally accelerated by increased aerobic respiration due to many factors such as concentrations of ethylene, O_2, and CO_2, together with the extending of infected lesions. These factors activated the enzymatic activities of α-amylase, β-amylase and invertase, leading to the breakdown of starch in mango fruit to glucose and fructose, and the result of increasing TSS. Afterwards, these sugars are used as respiratory substrates or further

converted to other metabolites (Paliyath & Murr, 2008), resulted in eventual decrease of TSS. In this case, ZE 0.2 can provide the same effect as modified atmosphere storage.

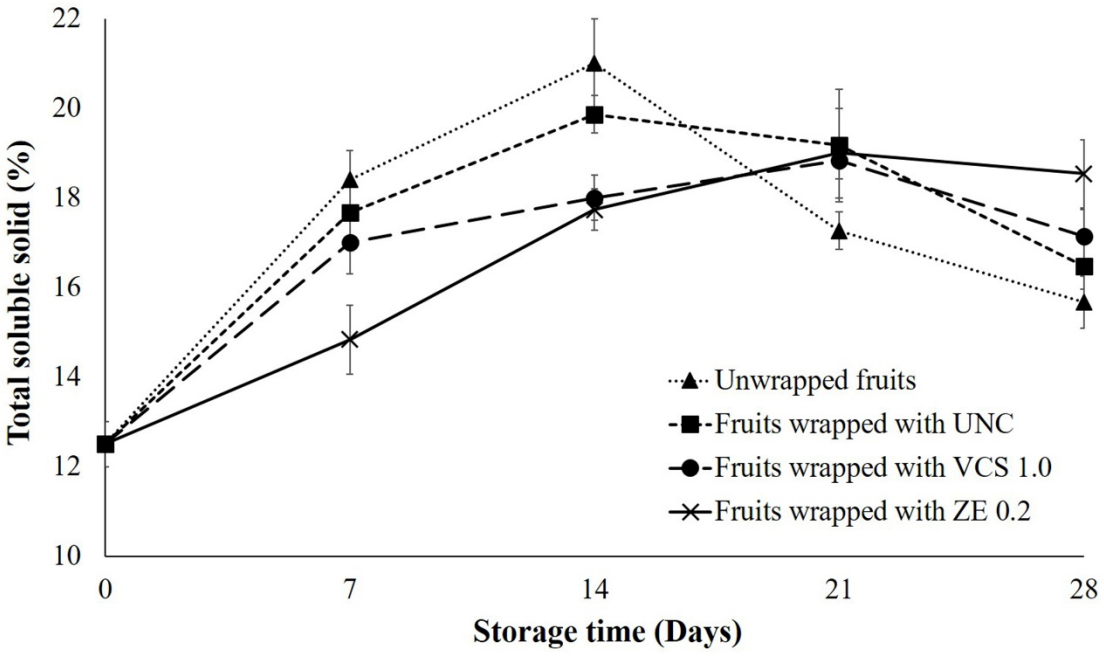

Figure 4.21 Changes in total soluble solid of mango fruits during storage at 13 °C for 28 days

4.5 Release Properties of Vanillin from Active-Coated Papers

4.5.1 Factors Affecting Release of Vanillin from Active-Coated Papers

In this study, the mechanism related to diffusion behavior for a plane sheet system with the average thickness of coating layer can be determined by fitting the diffusion curve ($M_t/M_\infty < 0.67$) to Equation (4.3) (Crank, 1975; Langer & Peppas, 1983; Peppas, 1985).

$$\frac{M_t}{M_\infty} = kt^n \tag{4.3}$$

Where, M_t/M_∞ is the fractional mass release of the vanillin, M_t is the amount of vanillin released at time t, M_∞ is the amount of vanillin released at equilibrium, t is the releasing time, k is a rate constant that characterizes the polymer network system (s^{-1}) and n is the diffusional exponent characteristic of the release mechanism. The diffusional exponent can be divided into 3 cases. Fickian diffusion (Case I system) is characterized by $n \leq 0.5$ which indicates that the rate of diffusion is much less than that of the film relaxation. Non-Fickian diffusion is denoted by $0.5 < n < 1.0$ which occurs when the diffusion and relaxation are comparable. The last case in which $n > 1$ indicates Super Case II system that diffusion is very rapid compared with the relaxation process of polymer (Crank, 1975; Choi et al., 2005). Values of n and k under different releasing conditions are shown in Table 4.9 which could be obtained from the slope and intercept of the ln M_t/M_∞ and ln t plot with the goodness of fit, $r^2 > 0.91$.

Under the different releasing temperatures, estimated n values were enhanced by increasing of temperatures and were in the range of 0.40 to 0.57. The kinetics of vanillin release showed a Fickian behavior at lower temperatures (13 to 25 °C) while the higher temperature (37 °C) showed a non-Fickian behavior. Likewise, the increasing RH also resulted in higher n values which ranged from 0.37 to 0.39, indicating that the Fickian diffusion is the predominant mechanism of vanillin release under RH effects whereas estimated n values for pH effect were decreased by increasing pH. They were in the range of 0.60 to 0.81, indicating that the non-Fickian diffusion is the predominant mechanism of vanillin release.

Table 4.9 Diffusion exponents (*n* value) and kinetic constants (*k* value) of the vanillin release under different releasing conditions

Variable factors	Fixed factors	*n* value	*k* value ($\times 10^{-5}$ s^{-1})	R^2
13 °C	Saturated salt solution of potassium nitrate (90 – 95 % RH)	0.40	3.33	0.99
25 °C		0.44	3.60	0.99
37 °C		0.57	4.07	0.99
75 % RH	13 °C	0.37	2.14	0.97
86 % RH		0.37	2.28	0.98
96 % RH		0.39	2.60	0.99
pH 3.8	13 °C	0.81	9.74	0.97
pH 5.2		0.77	6.58	0.98
pH 6.2		0.60	4.17	0.99

Under different releasing solvents, different mechanisms were found in the release of vanillin from ZE 0.2. Values of *n* and *k* are shown in Table 4.10 in which the r^2 values of their linearity plots between ln M_t/M_∞ and ln *t* are more than 0.97. ZE 0.2 immersed in water, 10 % ethanol, and 3 % acetic acid exhibited the higher *n* values (0.44 to 0.81) when the solvent temperature was higher. Differed from release of vanillin in olive oil in which *n* values were reduced by increasing of the solvent temperature (0.14 to 0.13). ZE 0.2 immersed in water, 10 % ethanol, and 3 % acetic acid under 25 and 37 °C had high *n* values, which showed non-Fickian diffusion. While, ZE 0.2 immersed in water and 10 % ethanol at 13 °C had low *n* values, which were possible that Fickian diffusion might be the predominant mechanism for this vanillin release.

Table 4.10 Effects of released solvents on diffusion exponents (n) and constants (k) of vanillin release

Released solvents	Temperature (°C)	n	k ($\times 10^{-5}$ s^{-1})	r^2
Water	13	0.47	6.09	0.99
	25	0.53	8.19	0.99
	37	0.63	9.05	0.98
10 % Ethanol	13	0.44	6.51	0.99
	25	0.52	8.11	0.99
	37	0.64	9.08	0.99
3 % Acetic acid	13	0.71	6.55	0.99
	25	0.79	6.87	0.99
	37	0.81	8.14	0.98
Olive oil	13	0.14	7.60	0.97
	25	0.13	8.05	0.97
	37	0.13	9.32	0.97

4.5.2 Comparison of Experimental Data with Theoretically Calculated Values

Figure 4.22 to 4.24 represent the release profiles of vanillin from active-coated paper. The fractional mass release (M_t/M_∞) as a function of the square root of time ($t_{0.5}$) can be calculated from Equation (4.4), using the D value was calculated from Equation (4.5) (Crank, 1975).

$$\frac{M_t}{M_\infty} = 1 - \frac{8}{\pi^2} \sum_{n=1}^{\infty} \frac{1}{(2n+1)^2} \exp\left[\frac{-(2n+1)^2 \pi^2 Dt}{l^2}\right] \tag{4.4}$$

$$D = \frac{0.049 \cdot l^2}{t_{0.5}} \tag{4.5}$$

Where, D value is the diffusion coefficient (cm^2/s), l is the thickness of coating layer on the active-coated paper. $t_{0.5}$ is the time when M_t/M_∞ equals to 0.5 (h). In this study, $t_{0.5}$ was determined from the linear of the initial portion of the curve that was plotted between M_t/M_∞ and $t_{0.5}$ in the range of a linear with good r^2 (> 0.90) (*i.e.*, $M_t/M_\infty < 0.67$).

Comparison of the experimental data with the theoretical data was done by using determination of correlation coefficient (r^2) between them which is represented in Figure 4.22 to 4.24. The obtained result showed a good agreement with good r^2 (> 0.90).

4.5.3 Effect of Temperature on the Releasing Profile of Vanillin

Figure 4.22 exhibits the releasing profiles for vanillin in ZE 0.2 under different temperatures which were fitted as a function of the square root of storage time. Increasing the temperature from 13 to 37 °C obviously caused a faster rate for the release of vanillin which could also reach the equilibrium faster than those at lower temperature. For the kinetic constant (k value) (Table 4.9) of the vanillin release from active-coated paper, this value was determined by Equation (4.3) in which the k value enhanced from 3.33×10^{-5} to 4.07×10^{-5} s^{-1}, and likewise, the diffusion coefficient (D value) (see Table 4.11) of vanillin through active-coated paper calculated with Equation (4.5) also enhanced from 78.24×10^{-10} to 162.10×10^{-10} cm^2/s ($p \leq 0.05$), when the temperature was increased from 13 to 37 °C. The time ($t_{0.5}$) required to release half amount of vanillin contained initially in the active-coated paper decreased from 2.23 to 1.10 h ($p \leq 0.05$), as shown in Table 4.11. This result demonstrated that the release of vanillin through chitosan matrix was accelerated with increasing temperature. Under the atmosphere with high RH (90 % RH), temperature effect on release of vanillin is well explained by a glass transition phenomenon. The glass transition temperature (T_g) of a polymeric matrix is one of the important physicochemical properties of the matrix. The polymeric matrix exists in a soft rubbery state above T_g and changes to a hard or brittle structure of the glassy state below T_g. The permeability properties of polymer materials are higher in the rubbery state (above T_g) where polymer chains are more mobile than in the glassy state (Gontard & Ring, 1996). In this study, the Tg of chitosan measured by using a differential scanning calorimetry (DSC) (TA Instruments, New Castle, DE, USA) was 10 °C, which was lower than the storage temperatures used in this study (13 to 37 °C). Therefore, chitosan-coating layers on the active-coated paper were expected to be rubbery.

The diffusivity of vanillin through rubbery chitosan-coating layer was enhanced by increasing temperature and led to an increment in the ability of the chitosan-coating layer to transport vanillin through its network. Sangsuwan et al. (2009) reported that temperature significantly impacted the release rate of vanillin from chitosan/methyl cellulose film, a faster release rate was observed as temperature increased. This is consistent with Ouattara et al. (2000), who demonstrated that increasing the temperature from 4 to 24 °C resulted in a faster rate of diffusion for acetic and propionic acids from chitosan-based films. Likewise, the similar result was also reported in some non-biopolymer films. Suppakul, Sonneveld, Bigger, and Miltz (2011) showed that an increase in temperature from 4 to 25 °C resulted in an increase in the diffusion coefficient of linalool and methylchavicol from low density polyethylene-based films. These results might be attributed to the change of free volume in films which response to temperature. The higher temperature caused the film swelling and resulted in bigger pores on the film surface, which increased the effective diffusion area. These phenomena facilitated the solutes to transport through the free water region in the swollen film (Fang et al., 1998; Yoshizawa et al., 2005).

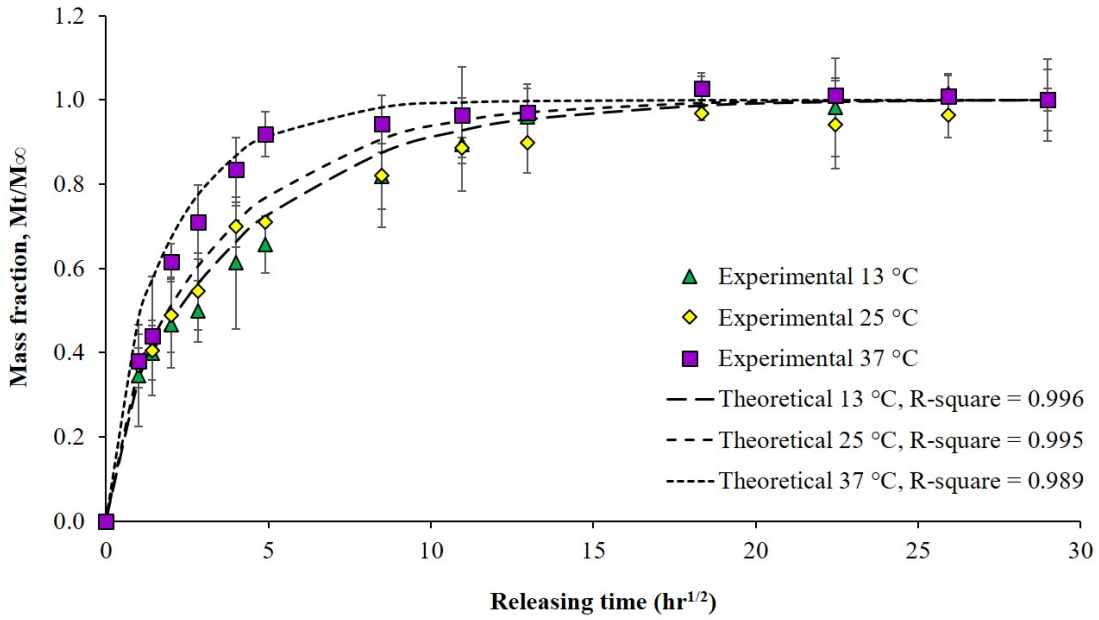

Figure 4.22 Releasing profiles for vanillin in ZE 0.2 under different temperatures

4.5.4 Effect of Relative Humidity on the Releasing Profile of Vanillin

Releasing profiles for vanillin in ZE 0.2 stored in the atmosphere with different RH are shown in Figure 4.23 which fitted as a function of the square root of storage time. The amount of released vanillin was enhanced by increasing RH, similar to the temperature effect. The $t_{0.5}$ values decreased from 4.05 to 2.89 h with increasing RH ($p \leq 0.05$). For the k values (Table 4.9) of the vanillin release from ZE 0.2, it was enhanced from 2.14×10^{-5} to 2.60×10^{-5} s^{-1}, and likewise, the D values (Table 4.11) was also enhanced from 42.87×10^{-10} to 59.98×10^{-10} cm^2/s ($p \leq 0.05$) when the RH was increased from 75 to 96 %. The results indicated that higher RH made the vanillin release reach the equilibrium faster. The addition or removal of water causes phase transition in the polymer structure, because of the chitosan's Tg is dependent on its water content providing the plasticizing effect (Ratto, Hatakeyama, & Blumstein, 1995; Lazaridou & Biliaderis, 2005; Rachtanapun & Wongchiya, 2012). Matveev, Grinberg, and Tolstoguzov (2000) explained that the plasticizing activity of water is the result of Tg reduction by reducing the inter- and intra-macromolecular forces. Additionally, its high dielectric constant and capability of strong interactions to other polar molecules leads to the formation of hydrogen bonds with many hydrophilic and charged groups of biopolymers resulting in the swollen film, which facilitate the transportation of solute.

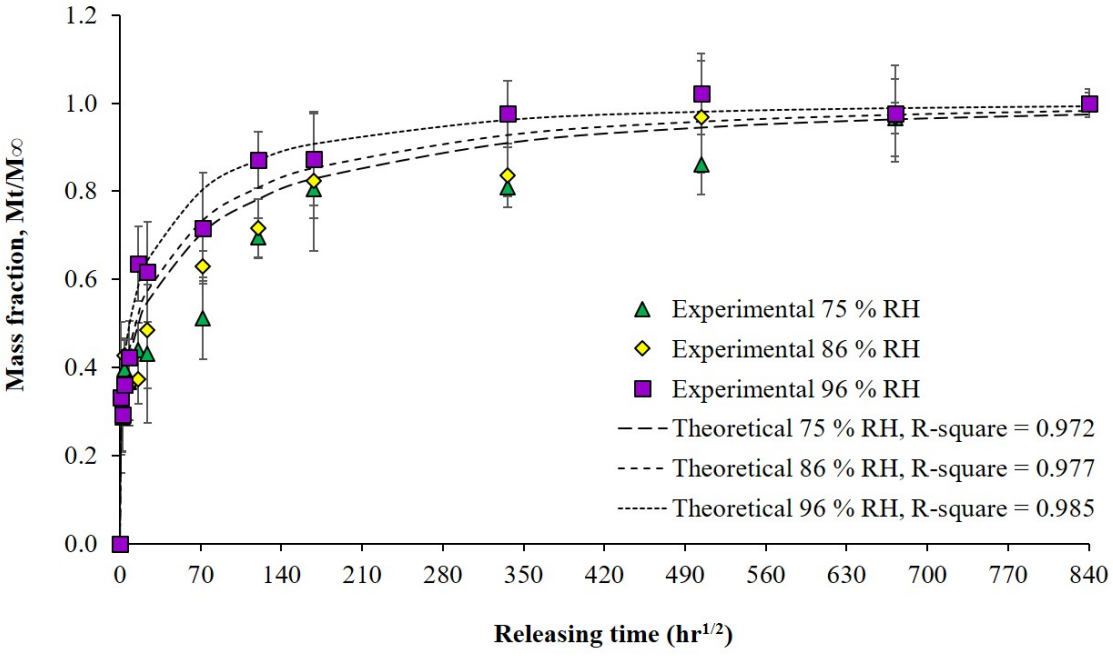

Figure 4.23 Releasing profiles for vanillin in ZE 0.2 under different RH conditions

In this study, the chitosan's Tg might be reduced by absorbing the water from the atmosphere with increasing RH, resulting in chitosan-coating layer was more sensitive to phase transition to be a rubbery state and easier to release vanillin. Thus the higher RH the greater vanillin release. Moreover, the combination effect of temperature and relative humidity can be strongly dependent on the diffusion coefficient. Increasing the storage temperature from 5 to 30 ºC and RH from 60 to 100 % resulted in an increase in carvacrol diffusivities from SPI-coated paper (Chalier et al., 2009). The influence of temperature and relative humidity on release was related to the glass transition phenomenon and its effect on chain polymer mobility and substances diffusivity. Therefore, the diffusion coefficient of substance increased as temperature and RH increased (Chalier et al., 2009).

4.5.5 Effect of Solvent pH on the Releasing Profile of Vanillin

Figure 4.24 exhibits the releasing profiles for vanillin in ZE 0.2 under the buffer solution with different pH values, which fitted as a function of the square root of storage time. Increasing of pH values from 3.8 to 6.2 caused a faster rate for the release of vanillin. The lower pH value facilitated the vanillin release, which could also be faster reached the equilibrium than those at the higher pH value (Figure 4.24) and the lowest $t_{0.5}$ was observed at pH 3.8 (0.75 h) and clearly increased to 1.46 h ($p \leq 0.05$) when the pH value increased to 6.2 (Table 4.11). For the k values release, this result showed that the release kinetic of vanillin from ZE 0.2 was considerably greater under the release condition of the buffer solution with pH 3.8 (9.74×10^{-5} s^{-1}) than other pH values, and decreased to 4.17×10^{-5} s^{-1} when pH increased as 6.2 (as seen in Table 4.9). Likewise, the D value of vanillin through ZE 0.2 also decreased from 233.87×10^{-10} to 122.74×10^{-10} cm^2/s ($p \leq 0.05$), when the pH value was increased from 3.8 to 6.2 (Table 4.11). Vanillin could diffuse from ZE 0.2 into the solution with pH 3.8 greater than pH 5.2 and pH 6.2 for 1 and 1.5 times, respectively. Corresponding with Sangsuwan et al. (2009), the authors found that the D values of vanillin moved from chitosan/methyl cellulose film to the citrate buffer were enhanced with decreasing pH. More vanillin migrated into citrate buffer pH 3.5 than citrate buffer pH 6.5 under the same concentration of acid. The swelling of chitosan-coating layer on active-coated paper might contributed to the release of vanillin. The lower pH value causes more swelling ratio of chitosan films than higher pH value (Shu et al., 2001; Yoshizawa

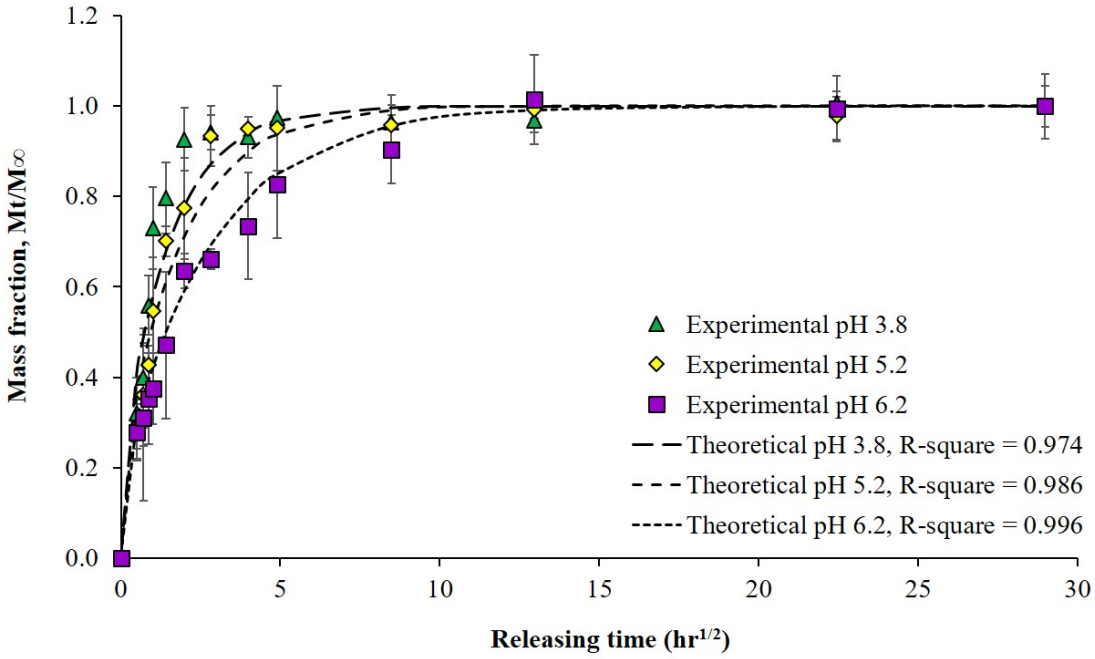

Figure 4.24 Releasing profiles for vanillin in ZE 0.2 under different pH conditions

Table 4.11 Diffusivity of vanillin under different release conditions

Variable factors	Control factors	$t_{0.5}$ (h)	D value ($\times 10^{-10}$ cm^2/s)
13 °C	Saturated salt solution of potassium nitrate (90 – 95 % RH)	2.23 ^{a} ± 0.28	78.24 ^{b} ± 10.60
25 °C		1.90 ^{a} ± 0.03	90.95 ^{b} ± 1.24
37 °C		1.10 ^{b} ± 0.24	162.10 ^{a} ± 36.59
75 % RH	13 °C	4.05 ^{a} ± 0.37	42.87 ^{b} ± 3.72
86 % RH		3.71 ^{a} ± 0.34	46.88 ^{b} ± 4.53
96 % RH		2.89 ^{b} ± 0.18	59.98 ^{a} ± 3.92
pH 3.8	13 °C	0.75 ^{b} ± 0.10	233.87 ^{a} ± 31.73
pH 5.2		0.94 ^{b} ± 0.09	185.12 ^{a} ± 18.16
pH 6.2		1.46 ^{a} ± 0.35	122.74 ^{b} ± 27.45

Data shows the average ± standard deviation of 3 replications (n = 3).

Different superscript letters for the same variable factor indicate significant difference at $p \leq 0.05$.

et al., 2005; Sangsuwan et al., 2009). The decrease in pH weakened salt bonds and therefore facilitated the swelling of film. Additionally, chitosan contained large amino groups that could absorb more proton (H^+) from acidic solution, leading to the formation of positively-charged ammonium ion ($-NH_3^+$) (Xie, Xu, & Liu, 2001). This phenomenon led to swelling of the chitosan-coating layer at low pH value and finally releasing of more vanillin.

4.5.6 Temperature Dependent of Diffusivity in Different Released Solvents

Releasing profiles for vanillin in ZE 0.2 immersed in different solvents including water, 10 % ethanol, 3 % acetic acid, and olive oil under various temperatures (13, 25, and 37 °C) are shown in Figure 4.25 to 4.28, respectively. For all solvents, the releasing profiles for vanillin in ZE 0.2 fitted as a function of the square root of storage time. The amount of released vanillin enhanced by increasing of temperature of water, 10 % ethanol, and 3 % acetic acid. Only olive oil where the amount of released vanillin slightly decreased by increasing of temperature. Confirmed from the release kinetic, values of k for water, 10 % ethanol, 3 % acetic acid, and olive oil increased from 6.09×10^{-5} to 9.05×10^{-5} s^{-1}, 6.51×10^{-5} to 9.08×10^{-5} s^{-1}, 6.55×10^{-5} to 8.14×10^{-5} s^{-1}, and 7.60×10^{-5} to 9.32×10^{-5} s^{-1} by increasing of temperature from 13 to 37 °C (Table 4.10).

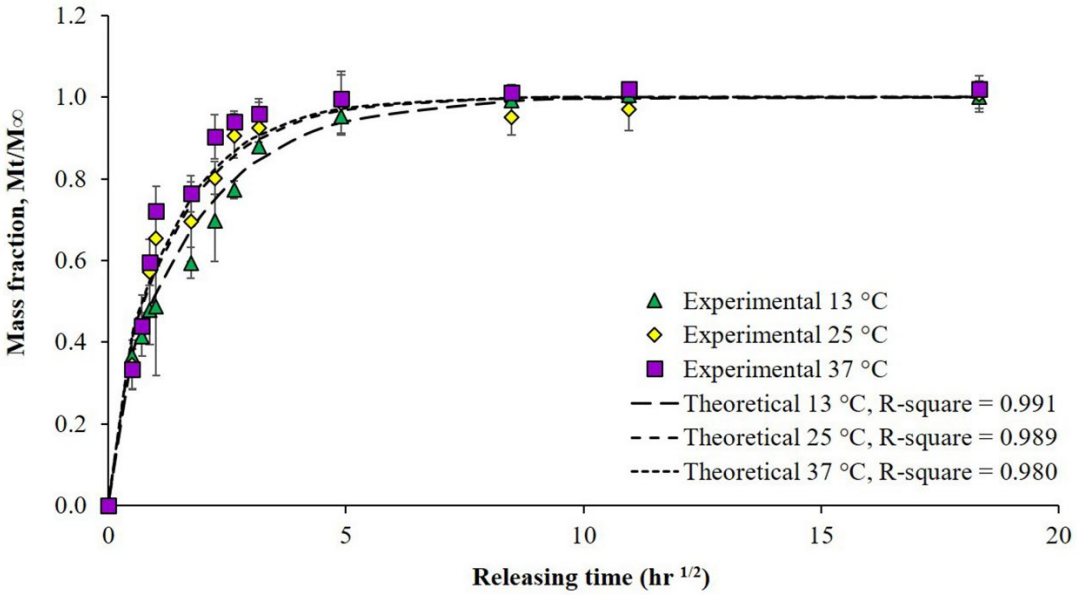

Figure 4.25 Releasing profile for vanillin in ZE 0.2 that immersed in water under various temperatures.

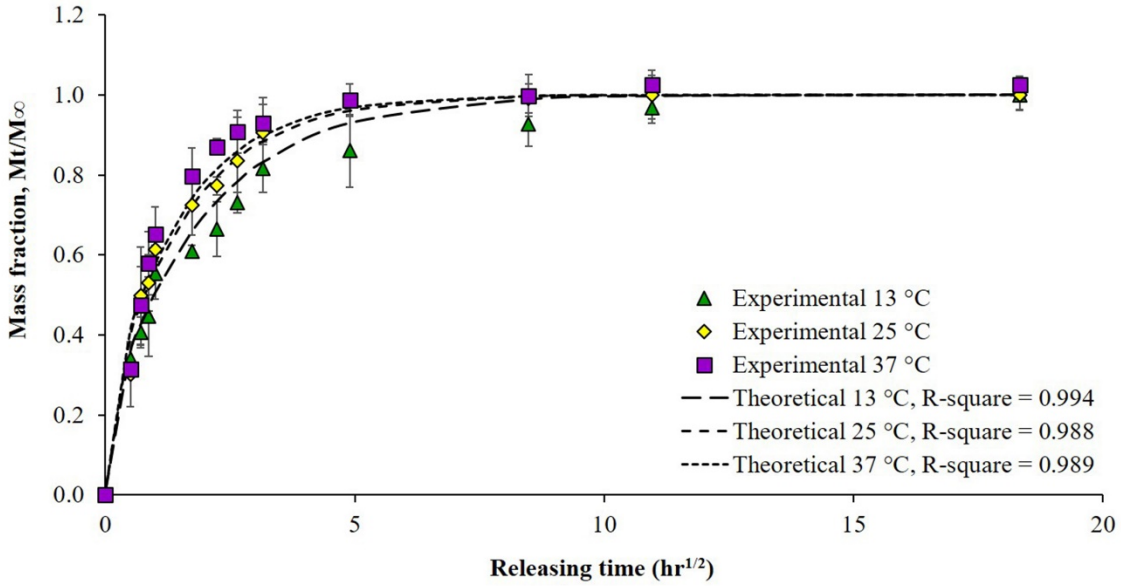

Figure 4.26 Releasing profile for vanillin in ZE 0.2 that immersed in 10 % ethanol under various temperatures.

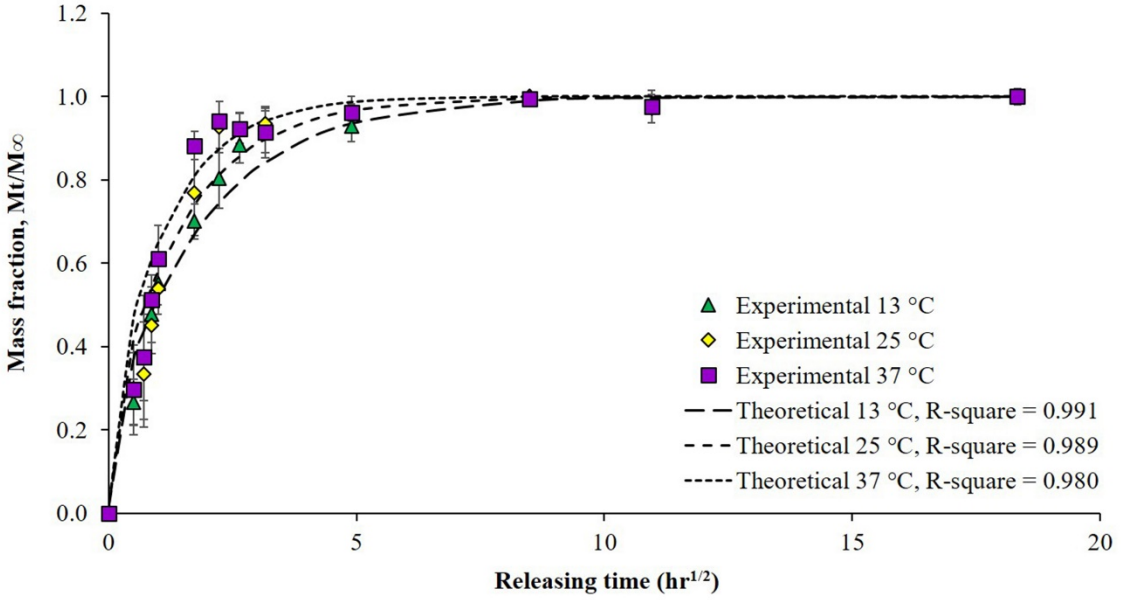

Figure 4.27 Releasing profile for vanillin in ZE 0.2 that immersed in 3 % acetic acid under various temperatures.

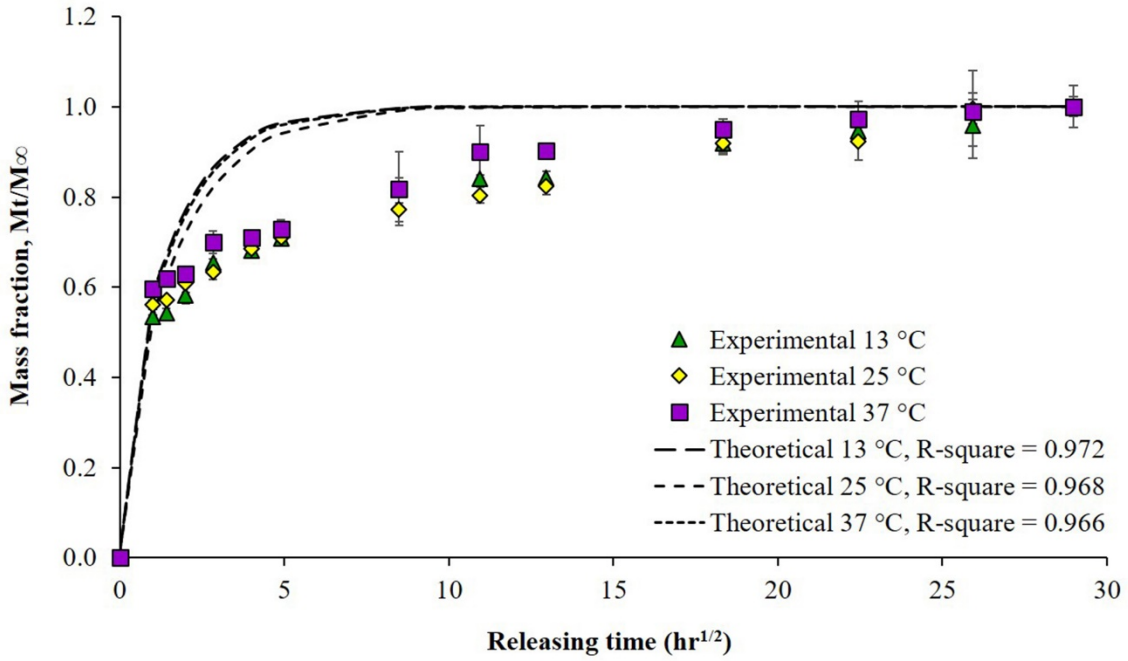

Figure 4.28 Releasing profile for vanillin in ZE 0.2 that immersed in an olive oil under various temperatures.

Table 4.12 Effects of releasing solvents on diffusion coefficient of vanillin release

Releasing solvents	Diffusion coefficient, × 10^{-10} cm^2/s)		
	13 °C	25 °C	37 °C
Water	181.06 ^{ab,B} ± 19.82	232.14 ^{a,A} ± 19.59	242.70 ^{a,A} ± 11.87
10 % Ethanol	177.40 ^{b,B} ± 15.86	219.41 ^{a,AB} ± 19.99	235.46 ^{a,A} ± 34.14
3 % Acetic acid	184.34 ^{ab,A} ± 19.36	233.94 ^{a,A} ± 42.93	296.71 ^{a,A} ± 82.14
Olive oil	190.15 ^{a,A} ± 25.95	216.75 ^{a,A} ± 19.17	225.23 ^{a,A} ± 22.76

Data shows the average ± standard deviation of 3 replications (n = 3).

Different lower case superscript letters, $^{a-b}$, in each column indicate the significant difference at $p \leq 0.05$.

Different upper case superscript letters, $^{A-B}$, in each row indicate the significant difference at $p \leq 0.05$.

The calculated D values for this experiment were summarized in Table 4.12. The increase in temperature from 13 to 37 °C significantly increased the diffusion of vanillin into water and 10 % ethanol ($p \leq 0.05$), which were in ranges of 181.06×10^{-10} to

242.70×10^{-10} cm^2/s and 177.40×10^{-10} to 235.46×10^{-10} cm^2/s, respectively. Whereas the increase in temperature from 13 to 37 °C had no significant effect on the diffusion of vanillin into 3 % acetic acid and olive oil ($p > 0.05$), which were in ranges of 184.34×10^{-10} to 296.71×10^{-10} cm^2/s and 190.15×10^{-10} to 225.23×10^{-10} cm^2/s, respectively. Under the higher temperature, vanillin in ZE 0.2 were released into the solvents at the higher releasing rate due to higher molecular mobility of polymer matrix. At the same temperature, there were not significant differences in the diffusivity of vanillin in ZE 0.2 into all solvents at 13 and 25 °C. However, the relatively high diffusivity was found when vanillin in ZE 0.2 released into 3 % acetic acid at 37 °C. Corresponding to the previous experiment, it is possible to be the effect of solvent's acidity. Under an acidic solution (or low pH value), large amino groups of chitosan can absorb more H^+ leading to the formation of NH_3^+ and more swelling ratio (Xie et al., 2001; Shu et al., 2001; Yoshizawa et al., 2005; Sangsuwan et al., 2009). Thus, the acidic solution of 3 % acetic acid might cause the swelling of chitosan-coating layer on active-coated paper, and resulting in more vanillin release than other solvents especially at higher temperature.

The influence of temperature on diffusivity of vanillin in ZE 0.2 could be described by the activation energy (*Ea*) which can be determined using Arrhenius plots derived from logarithmic transform of Equation (4.6). Slope of the ln *D* and 1/*T* plots were used to calculate the activation energy. The greater *Ea* indicates the diffusivity is more sensitive to change of temperature (Choi et al., 2005; Sangsuwan et al., 2008).

$$D = D_0 \exp\left(-\frac{Ea}{RT}\right) \tag{4.6}$$

Where, *D* is the diffusion coefficient, D_0 is a constant, *Ea* is the activation energy for the diffusion process (kJ/mol), *R* is universal gas constant equal to 8.314 J/K·mol, and *T* is absolute temperature (K). The obtained *Ea* and D_0 for all of the studied solvents was shown in Figure 4.29. *Ea* values of ZE 0.2 in water, 10 % ethanol, 3 % acetic acid, and olive oil were 8.20, 8.63, 14.01, and 5.33 kJ/mol, respectively. While, D_0 values of ZE 0.2 in water, 10 % ethanol, 3 % acetic acid, and olive oil were 0.60×10^{-6}, 0.68×10^{-6}, 6.61×10^{-6}, and 0.18×10^{-6} cm^2/s, respectively.

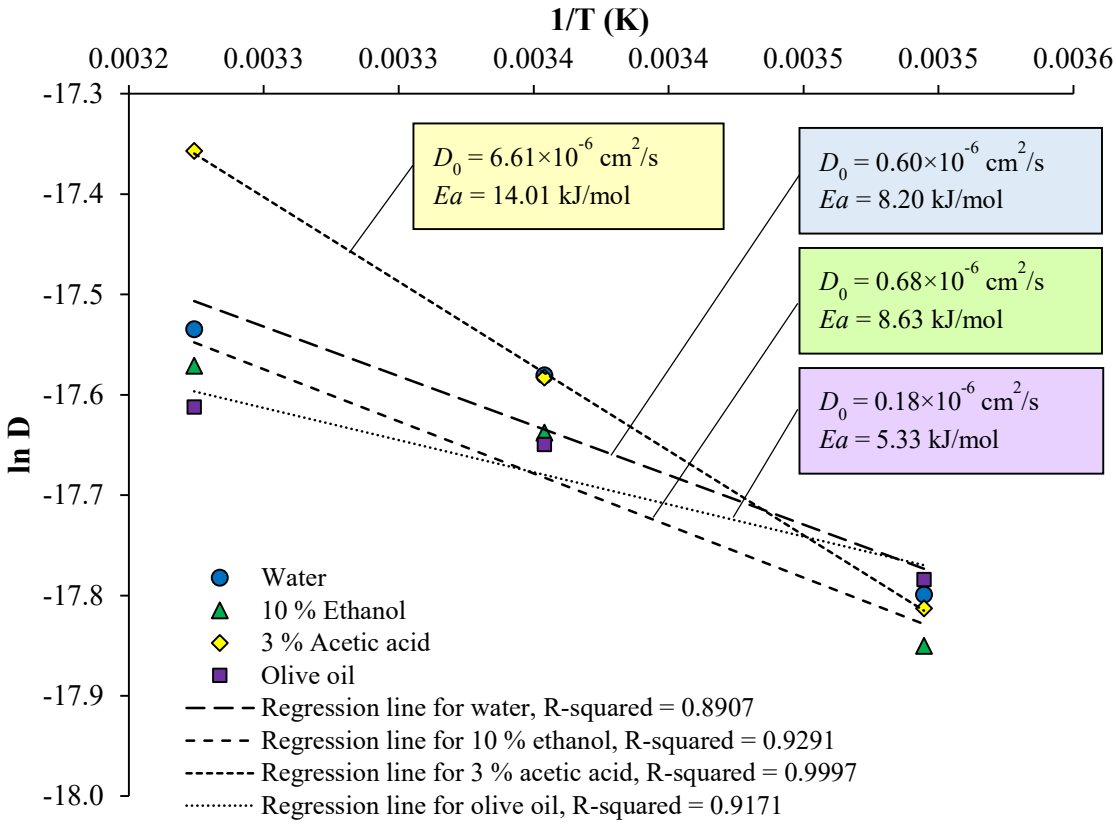

Figure 4.29 Arrhenius plots of ZE 0.2 in water, 10 % ethanol, 3 % acetic acid, and olive oil at 13, 25, and 37 °C

As shown in Figure 4.29, the result indicated that release of vanillin into 3 % acetic acid was most sensitive to the temperature change, while the lowest sensitivity to temperature change was observed in olive oil. This result might be the effect of acidity which caused the swelling of chitosan structure, facilitating the migration of vanillin. The H^+ existing in acidic solution can be absorbed by amino groups of chitosan (Xie et al., 2001), and lead to the swelling of chitosan structure through an electrostatic repulsion between NH_3^+ groups. Shu et al. (2001) and Yoshizawa et al. (2005) reported that amino groups in chitosan film were in the form of NH_3^+ at low pH and caused film swelling which led to the higher leaching of migrant from the chitosan network. Water, 10 % ethanol, and olive oil do not have H^+ like 3 % acetic acid. Moreover, the effect of water on polymer chain mobility plays an important role on diffusivity of vanillin from the network of chitosan coating layers. The plasticization by water caused the polymer chain more mobile and increasing in free volume, leading to an increment in the ability of small molecules such as aroma compounds transport through polymer's network (Chalier et al.,

2009; Mascheroni, Guillard, Gastaldi, Gontard, & Chalier, 2011). This phenomenon rendered the swelling of the chitosan-coating layer in water and 10 % ethanol greater than in that in oil. Although water facilitates vanillin to move through the chitosan matrix, the release of vanillin into 10 % ethanol was more sensitive to the temperature change than water. It is well-known that the relative polarity of ethanol (0.654) was lower than water (1.000) (Semsri, Ampasavate, Okonogi, Srikamchum, & Anuchapreeda, 2009). Thus, the lower polarity of 10 % ethanol than water might be contributed to more sensitivity to temperature change for vanillin release, due to its hydrophobicity of vanillin (Sangsuwan et al., 2009). While, very low polarity of the olive oil caused the lowest vanillin release, due to its poor hydrophilicity. The influence of temperature on diffusion can be explained by effects on the solubility of diffusing molecules in films, on the nature of adhesive forces at interfaces, and on molecular mobility (Vojdani & Torres, 1990; Myint, Daud, Mohamad, & Kadhum, 1996). Diffusion can be described by an Arrhenius equation which suggests that the effect of temperature is thermodynamic in nature and controlled by the ratio of energy provided to *Ea*. Tg of a polymeric matrix is one of the important physicochemical properties, which is soft and rubbery above Tg and hard or brittle below Tg. Therefore, above Tg the molecular mobility in a system increases with temperature, which leads to an increment in the ability of the vanillin to transport through the chitosan network.

4.5.7 Release of Vanillin on Mango Fruits Wrapped by ZE 0.2

At the beginning, the active wrapping paper contained an initial amount of vanillin equal to 193.82 μg/mL, which was continuously reduced by increasing storage time as seen in Figure 4.30 (A). At the end (840 h), the remaining vanillin in the paper was 42.25 ± 12.89 μg/mL (21.20%), or that is, vanillin released from the paper to the surface of mango fruit was approximately 151.57 ± 13.67 μg/mL (78.20 %). Figure 4.30 (B) exhibits the releasing profile of vanillin from active wrapping paper which wrapped a mango fruit under an actual wrapping condition of commercial fruit, which fitted as a function of the square root of storage time. The estimated *n* value was 0.27 (r^2 = 0.88) which showed a Fickian behavior as the predominant mechanism of vanillin release. This *n* value obtained might be related to the air movement around fruits, which were limited by the wrapping paper and caused an accumulation of the water vapor surrounding the fruit and difficult to disperse out. The water accumulation around the fruit wet the wrapping paper. Thus

this experiment had the lower *n* value and the higher *k* value than the previous experiment that studied the temperature or RH effects. The *k* and *D* values of vanillin release from active wrapping papers that wrapped mango fruits were 5.17×10^{-5} s^{-1} and 65.36×10^{-12} cm^2/s respectively, which was relatively slower than release of vanillin under different temperatures or RH values studied in the previous section. The diffusion of vanillin from coated paper in previous section was studied in a big chamber under various temperature and RH. In chamber, the concentration gradient of vanillin between active wrapping paper and surrounding air was relatively high, resulting in the freely release of vanillin out of the coated paper. While, the release of vanillin from coated paper that wrapped around the mango fruit was slower because the space surrounding the mango fruit was limited, leading to the accumulation of vanillin vapor and might cause the reduction of concentration gradient. However, slower release of vanillin from active wrapping papers might expand the period of microbial inhibition in wrapped mango fruits.

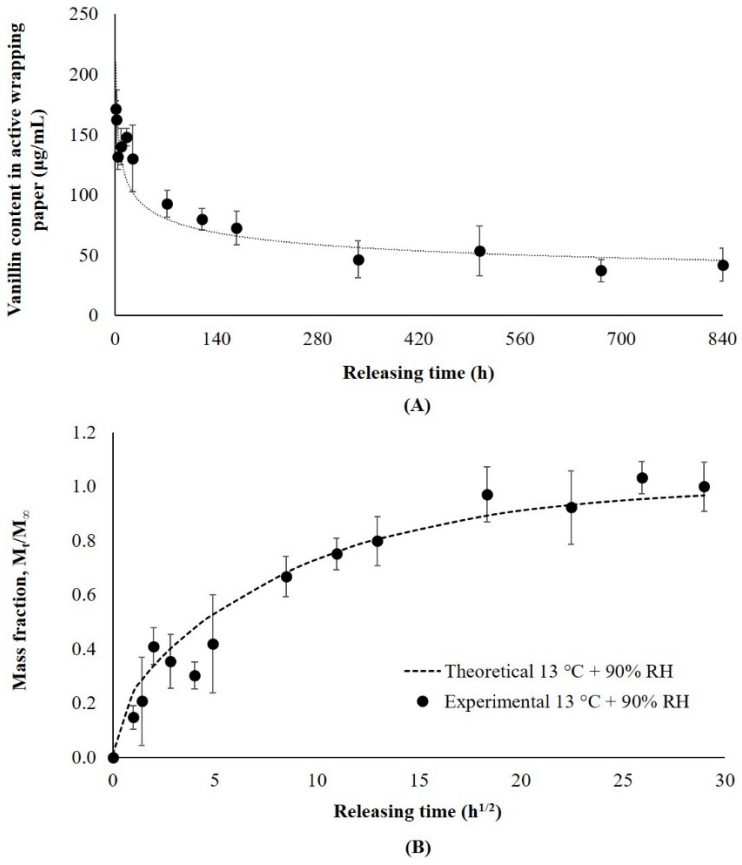

Figure 4.30 Releasing profiles for vanillin in ZE 0.2, which applied to wrap a mango fruit.